arXiv:1411.3709v2 [q-bio.PE] 14 Nov 2014

A general condition for adaptive genetic polymorphism in temporally and spatially heterogeneous environments

Hannes Svardal [2,3,6], Claus Rueffler [2,4,7] and Joachim Hermisson [2,5,8]

[2]*Mathematics and Biosciences Group, Department of Mathematics, University of Vienna, 1090 Vienna, Austria*

[3]*present address: Gregor Mendel Institute, Austrian Academy of Sciences, 1030 Vienna, Austria*

[4]*Animal Ecology, Department of Ecology and Genetics, Uppsala University, 752 36 Uppsala, Sweden*

[5]*Max F. Perutz Laboratories, 1030 Vienna, Austria*

ABSTRACT

Both evolution and ecology have long been concerned with the impact of variable environmental conditions on observed levels of genetic diversity within and between species. We model the evolution of a quantitative trait under selection that fluctuates in space and time, and derive an analytical condition for when these fluctuations promote genetic diversification. As ecological scenario we use a generalized island model with soft selection within patches in which we incorporate generation overlap. We allow for arbitrary fluctuations in the environment including spatio-temporal correlations and any functional form of selection on the trait. Using the concepts of invasion fitness and evolutionary branching, we derive a simple and transparent condition for the adaptive evolution and maintenance of genetic diversity. This condition relates the strength of selection within patches to expectations and variances in the environmental conditions across space and time. Our results unify, clarify, and extend a number of previous results on the evolution and maintenance of genetic variation under fluctuating selection. Individual-based simulations show that our results are independent of the details of the genetic architecture and on whether reproduction is clonal or sexual. The onset of increased genetic variance is predicted accurately also in small populations in which alleles can go extinct due to environmental stochasticity.

Subject headings: evolutionary branching, coexistence, frequency dependence, island model, lottery model, soft selection

[6]corresponding author: hannes@svardal.at

[7]claus.rueffler@ebc.uu.se

[8]joachim.hermisson@univie.ac.at

1. Introduction

Explaining observed levels of genetic variation within natural populations is one of the major challenges in the study of evolution. One can distinguish adaptive explanations from non-adaptive explanations, with neutral variation and mutation-selection balance being the prime examples for the latter. Amongst adaptive explanations we can distinguish those based on genetic constraints such as over-dominance, where only heterozygote individuals can realize highest fitness, from those that do not rely on such constraints and consequently also apply to haploid species. In the latter case, genetic diversity is an adaptive response to the environment. Our aim is to characterize the conditions that select for adaptive diversity in this sense.

Both temporal and spatial fluctuations are omnipresent in natural populations. From early on there has been a perception in evolutionary research that such fluctuations should be favorable for the evolution and maintenance of genetic diversity. Modelling efforts to support this claim started in the second half of the 20th century (reviewed in Felsenstein 1976 and Hedrick et al. 1976). Spatial heterogeneity was soon identified as a potent factor to maintain diversity, even if individuals move freely among patches. The pioneering model here is the Levene model (Levene 1953; Gliddon and Strobeck 1975), an island model (Wright 1943) with different selective pressures among islands (or patches) and random dispersal of all individuals in each generation. As pointed out by Dempster (1955), a crucial feature of the Levene model is that density regulation takes place locally within patches. This "soft-selection" regime (Wallace 1975; Christiansen 1975) can adaptively maintain a protected genetic polymorphism. If only a part of the population disperses, this further aids the maintenance of genetic variation as sub-populations can become locally adapted (Deakin 1966, 1968; Spichtig and Kawecki 2004).

In the absence of genetic constraints, it was initially thought that purely temporal fluctuations in selection are not sufficient to maintain genetic polymorphism, but would generally favor the genotype with the highest geometric mean fitness (Gillespie 1973*b*, 1974; Felsenstein 1976). It was therefore concluded that temporal fluctuations can only account for a limited amount of the observed genetic variance in diploid populations (Dempster 1955) and that there is no tendency to maintain polymorphism in haploid populations (Cook and Hartl 1974). However, two mechanisms were subsequently identified that can maintain genetic polymorphism under temporal fluctuations, named the "storage effect of generation overlap" (Chesson and Warner 1981; Chesson 1984) and the "effect of relative non-linearity" (Chesson 1994; Szilagyi and Meszena 2010). In both cases, selection is no longer a function of time alone: With the storage effect, selection acts only on a short-lived stage of the life cycle (e.g., juveniles), while a long-lived stage (e.g., adults or persistent dormant stages) is not affected by the fluctuations. With the non-linearity effect, temporal fluctuations lead to fluctuations in the population density and polymorphism is maintained by an additional density-dependent selection component.

Environmental heterogeneities simultaneously occurring in space and time have also been studied. After an early attempt by Levins (1962), it was mainly Gillespie (1974, 1975, 1976; but see also

Hedrick 1978) who treated this topic. He considered fluctuations in an island model, in which the distribution of environmental conditions is identical across all patches, but in which the realized environment at any given point in time may differ among patches. Gillespie's main conclusion was that these transient spatial differences can be sufficient to maintain genetic diversity.

Adaptive maintenance of genetic diversity can also be addressed from an ecological perspective, where species coexistence is a classical research focus (see Chesson 2000*b* for a review). Models and methods are closely related to their genetic counterparts, although this connection is often not made explicit. For clonal inheritance, it is only a matter of semantics whether maintenance of polymorphism within species (population genetics) or species diversity (ecology) is considered. Conditions for species coexistence in temporally and spatially fluctuating environments have been studied by Chesson (1985, 2000*a*) and Comins and Noble (1985). Both combine an island model with environmental fluctuations in time and space (similar to Gillespie's model) with Chesson's lottery model introducing generation overlap. They find that in such a scenario both temporal and spatial environmental fluctuations can promote species coexsistence.

Most models described above focus on the maintenance of diversity among two discrete and immutable alleles or types. Thus, stability of the polymorphism is considered from the short-term evolutionary perspective of the dynamics of allele (or phenotype) frequencies. From a long-term evolutionary perspective, one can further ask whether a polymorphism remains stable also in the presence of mutations leading to gradual adaptive changes in the allelic values or phenotypes. In particular, evolutionary stability in this sense should also guarantee that the polymorphism cannot be lost due to the appearance of a single superior (generalist) type. This long-term evolutionary stability has increasingly gained attention with the development of adaptive dynamics and the discovery of evolutionary branching points (Metz et al. 1992, 1996; Dieckmann and Law 1996; Geritz et al. 1998). Evolutionary branching points are trait values that are attractors of the evolutionary dynamics, but once the population has evolved sufficiently close to such trait values, selection turns disruptive and alternative alleles can invade and coexist. In short, evolutionary branching indicates that the emergence and maintenance of genetic polymorphism is an adaptive process. Several recent studies have used this approach to ask how environmental heterogeneity affects the existence of evolutionary branching points. This has been done for purely spatial heterogeneity (Meszéna et al. 1997; Geritz et al. 1998; Day 2000; Nilsson and Ripa 2010*a*,*b*), under purely temporal variation (Ellner and Hairston 1994; Svardal et al. 2011; Abrams et al. 2013) and for a combination of the two (Kisdi 2002; Parvinen and Egas 2004; Nurmi and Parvinen 2008, 2011). Note that the latter studies by Parvinen and coworkers are meta-population models in which temporal variation is introduced through catastrophes wiping out local populations. The general conclusion from the above studies is that in spatially heterogeneous environments low migration and large spatial differences favor evolutionary branching, while under purely temporal fluctuations a sufficiently large generation overlap is necessary for branching.

In this article, we follow the recent line of research and ask how environmental heterogeneity affects the scope for the adaptive evolution and maintenance of genetic polymorphism. We consider

a modified island model with local population regulation resulting in constant patch occupancies (soft selection), which combines features from the approaches above and extends them in several directions. We follow the evolution of a quantitative trait with a continuum of alleles. The strength and direction of selection within a patch depends on the realized environmental condition. In particular, we allow for an arbitrary distribution of environmental conditions across space and time, including spatial and temporal correlations. The functional dependence of fitness on the trait is also arbitrary. For example, selection can be stabilizing with the optimal trait value depending on the realized local environment, or directional with the direction fluctuating in space and time. We analytically derive a condition for the existence of an evolutionary branching point and investigate the robustness our finding with individual-based simulations.

2. Model

2.1. Population structure and life cycle

Consider the classical island model of population genetics (Wright 1943). A population occupies n patches that are connected by dispersal. We assume that the population dynamics is regulated locally by a limiting resource (e.g., space) so that the adult population size within each patch is at a stable equilibrium and stays constant over time. For our analytical treatment, we assume that local populations are sufficiently large so that stochastic effects due to drift can be ignored. This assumption is relaxed in section 3.6, where we present simulation results for small populations. For large populations, our results are independent of the total population size and it is sufficient to follow relative population sizes in the following.

The life cycle is shown in figure 1 and an overview of our notation can be found in table 1. The relative carrying capacity for adults may depend on the patch, with a fraction of k_i adults living in the ith patch, i.e., $\sum_{i=1}^{n} k_i = 1$. Adults reproduce within their patch and a fraction $1-\gamma$ dies after reproduction. The remaining fraction γ survives to the next reproductive season. Hence, we allow for overlapping generations and the parameter γ will be called "generation overlap" in the following. The case $\gamma = 0$ corresponds to the classical island model with non-overlapping generations and for $\gamma \to 1$ the individuals approach immortality. Note that the long-lived life-stage could also be a dormant stage such as resting eggs or a seed bank (Ellner and Hairston 1994).

Juveniles are subject to local viability selection, which depends on their phenotype and the realized environmental condition in the patch. After selection, trait-independent local density regulation further decreases offspring to a patch specific relative juvenile carrying capacity c_i, where $\sum_{i=1}^{n} c_i = 1$. A fraction m of the surviving offspring disperses globally so that the probability of arriving in a certain patch is independent of the patch of origin. This can be modeled as a common dispersal pool for the dispersing offspring of all patches. Note that this includes the possibility that dispersers return to their patch of origin. A fraction $1-m$ of juveniles stays in their native patch.

Offspring individuals are recruited to the adult population of patch i until its adult carrying capacity k_i is reached. The offspring population is assumed large enough so that this is always possible. Hence, a fraction $(1-\gamma)$ of the adults in each patch derive from the offspring of the previous reproductive season. New recruits are taken with equal probabilities from the non-dispersing offspring in patch i and the immigrants. All non-recruited juveniles die.

Table 1: Overview of the notation

m	probability that a juvenile individual disperses out of its native patch
γ	generation overlap; probability that an adult individual survives to the next reproductive season
k_i, c_i	relative adult and juvenile carrying capacity in patch i
y, x	trait values of the quantitative trait; under the adaptive dynamics approximation, y is the mutant trait value and x the resident trait value
x^*	trait value at which directional selection is zero on average (singular point)
$\phi_{it}(y)$	frequency of individuals with trait value y in patch i at time t
θ_{it}	environmental condition in patch i at time t
$r(y,\theta_{it})$	expected number of offspring before density regulation of an individual with trait value y under environmental condition θ_{it}
$\rho(y,\phi_{it},\theta_{it})$	relative reproductive success of an individual with trait value y in patch i at time t; under the adaptive dynamics approximation we write $\rho(y,x,\theta_{it})$ for the reproductive succes of a mutant individual with trait value y in a population with resident trait value x
s_{it}	$=\ln(\rho(y,x,\theta_{it}))$; local selection coefficent
$\partial s_{it}, \partial^2 s_{it}$	local selection gradient and local selection curvature evaluated at the singular point; $\frac{\partial s_{it}}{\partial y}\vert_{y=x=x^*}$ and $\frac{\partial^2 s_{it}}{\partial y^2}\vert_{y=x=x^*}$, respectively
$l_{ij}(y,\phi_{jt},\theta_{jt})$	expected contribution of individuals with trait value y from patch j to the adult population of patch i at the next time step; under the adaptive dynamics approximation we write $l_{ij}(y,x,\theta_{jt})$
$\mathsf{L}(y,\phi_{1t},..,\phi_{nt},\theta_{1t},..,\theta_{nt})$	population projection matrix with elements $l_{ij}(y,\phi_{jt},\theta_{jt})$; under the adaptive dynamics approximation we write $\mathsf{L}(y,x,\theta_{1t},...,\theta_{nt})$
$w(y,x)$	invasion fitness
$\mathrm{E_S}[.]$, $\mathrm{E_T}[.]$	spatial and temporal averages
$\mathrm{Var_S}[.]$, $\mathrm{Var_T}[.]$	spatial and temporal variances

2.2. Phenotypes and environments

Individuals are characterized by a quantitative trait that can take any value y in the real numbers. For concreteness, we assume that the trait is expressed in juveniles and affects juvenile viability, but our results also apply to a trait affecting adult fecundity (see *Discussion*). We denote

by ϕ_{it} the density function of individuals with different trait values in patch i at time t. Hence, $\phi_{it}(y)\mathrm{d}y$ is the frequency of individuals with a trait value between y and $y + \mathrm{d}y$ and we have $\int_{-\infty}^{\infty} \phi_{it}(y)\mathrm{d}y = 1$. For simplicity, we refer to $\phi_{it}(y)$ as frequency of individuals with trait value y in the following. We assume that genotypes uniquely map to phenotypes. Therefore, selection for phenotypic diversity at the trait level also selects for genetic diversity.

The condition of the environment in patch i at time t will be denoted by θ_{it}. In general, θ_{it}, can be a vector containing an arbitrary number of external environmental factors, such as temperature, humidity, or the presence/absence of a pathogen, each taking either continuous or discrete values. For simplicity, we will assume in the following that θ_{it} is scalar, but note that all our general derivations also holds for vector-valued θ_{it}. We refer to the realization of the environmental conditions in all patches at time t as environmental state and denote it by $(\theta_{1t}, .., \theta_{nt})$. The set of possible environmental states, i.e., the sample space, will be denoted by Ω. Our analytical treatment relies on the assumption that the probability for a certain environmental state does not explicitly depend on time. In other words, we assume a stationary distribution of environmental states and denote the probability density for environmental state $(\theta_1, .., \theta_n)$ by $f(\theta_1, .., \theta_n)$. For example, this is the case if the environmental states are determined by an ergodic Markov process. It follows that our formalism does not capture scenarios of prolonged directional change, such as global warming. However, our model allows for any form of spatial and temporal correlations in the environmental conditions.

2.3. Selection

We denote by $r(y, \theta_{it})$ the reproductive success, defined as the number of offspring after viability selection, of an individual with trait value y under environmental condition θ_{it}. Our main result holds for any function $r(y, \theta_{it})$. As a concrete example, we consider Gaussian stabilizing selection, where the scalar environmental condition θ_{it} determines the selective optimum for the trait,

$$r(y, \theta_{it}) = r_{\max} \exp\left[-\frac{(\theta_{it} - y)^2}{2\sigma^2}\right]. \tag{1}$$

Here, $r_{\max}$ is the maximal number of offspring. Given that it is the same for all individuals, it cancels out in the following. σ^2 parametrizes the strength of stabilizing selection. Note that small values of σ^2 correspond to strong selection and vice versa.

In a second step, the relative number of offspring in each patch is reduced by local density regulation (due to limitations in space or other resources) to the juvenile carrying capacity c_i. Importantly, the density-dependent reduction in total patch offspring is a trait-independent random sampling step so that the expected contribution of an adult individual from patch i to c_i is proportional to its reproductive success relative to the average reproductive success in the patch. We

denote an individual's relative reproductive success by

$$\rho(y, \phi_{it}, \theta_{it}) = \frac{r(y, \theta_{it})}{\int_{-\infty}^{\infty} \phi_{it}(x) r(x, \theta_{it}) \mathrm{d}x}, \tag{2}$$

where the integral in the denominator normalizes the reproductive success by the average reproductive success in the patch. Hence, we assume soft selection (Wallace 1975) and ρ depends on the local frequency distribution of all phenotypes, ϕ_{it}, in patch i at time t.

2.4. Dispersal

A fraction m of the offspring surviving density regulation disperses over the whole population. We assume that the number of migrants that each patch i contributes to and receives from the global migrant pool is proportional to its juvenile carrying capacity c_i. While being mathematically convenient, this choice is also biologically sensible. It means that the chance that an individual arrives in a certain patch is proportional to the resources this patch provides for offspring. Finally, from the non-dispersing offspring of patch i and the dispersing offspring that arrive in patch i, a random subset is selected to replace the fraction of $(1 - \gamma)$ deceased adults. All non-recruited offspring die. Note that out model allows the relative adult carrying capacity of a patch (k_i) and the relative number of juveniles it sends out and receives (c_i) to differ.

2.5. Dynamics

The frequency of adult individuals with trait value y in generation $t + 1$ is given by

$$\phi_{i,t+1}(y) = \sum_{j=1}^{n} l_{ij}(y, \phi_{jt}, \theta_{jt}) \phi_{jt}(y), \tag{3}$$

where l_{ij} are the elements of the population projection matrix $\mathsf{L}(y, \phi_{1t}, .., \phi_{nt}, \theta_{1t}, .., \theta_{nt})$. They are given by

$$l_{ij}(y, \phi_{jt}, \theta_{jt}) = (1 - \gamma) m c_j \rho(y, \phi_{jt}, \theta_{jt}) \text{ for } j \neq i \tag{4a}$$

$$l_{ii}(y, \phi_{jt}, \theta_{jt}) = \gamma + (1 - \gamma)\left(1 - m + m c_i\right) \rho(y, \phi_{it}, \theta_{it}) \tag{4b}$$

(appendix A). Each entry l_{ij} gives the expected contribution of individuals with trait value y from patch j to the adult population of patch i at the next time step. The term γ on the right-hand side of equation (4b) reflects the possibility that an adult can survive from one time step to the next. All other terms represent the recruitment of offspring to the adult population. By describing the adult population in terms of the relative frequency of individuals with a given trait value, rather than in absolute numbers, equations (3) and (4), and therefore all further derivations, become independent

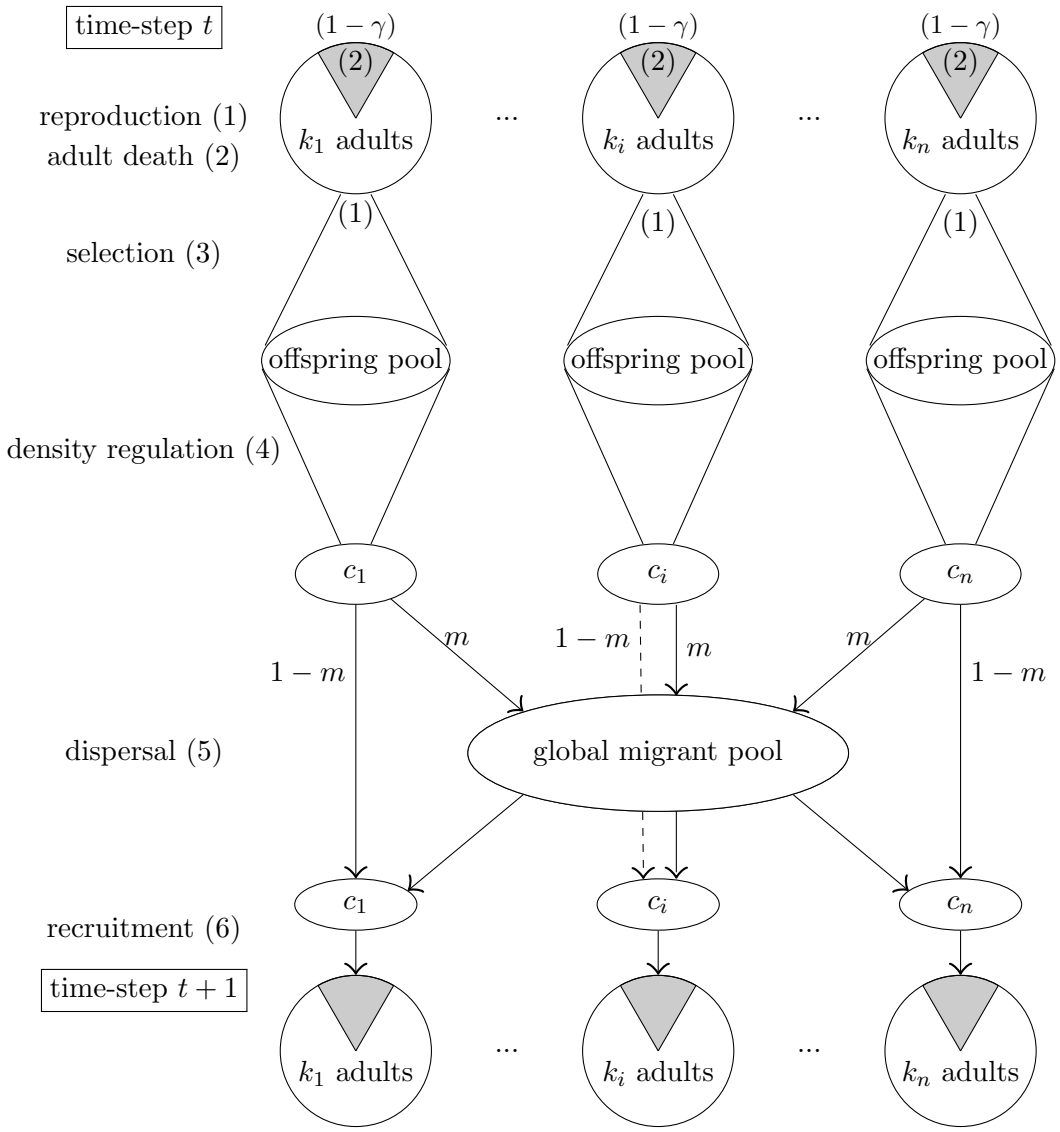

Fig. 1.— Life cycle: (1) reproduction, (2) adults die with probability $1-\gamma$, (3) viability selection on juveniles, dependent on trait and patch-specific environmental condition θ_{it}, (4) density regulation within patches resulting in the relative offspring contribution c_i, (5) a proportion $1-m$ of the offspring stays in the patch of origin, the rest contributes to a global migrant pool from where offspring are redistributed over all patches, (6) offspring replace the deceased adults and offspring that cannot establish die.

of the adult carrying capacities, k_i. Thus, our results will not depend on the relative patch sizes in the adult population.

In table 2 we list previously analyzed models with ecological settings that are special cases

of our model. Furthermore, the table gives the parameter values for which our ecological model becomes equivalent to the model in the reference.

Table 2: Previously analyzed models that are special cases of our model

reference	model assumptions in our notation	note
Levene (1953); Geritz et al. (1998)	$\gamma = 0$, $(\theta_1, .., \theta_n)$ fixed over time, $m = 1$	Levene model, see appendix C.3
Deakin (1966)	$\gamma = 0$, $(\theta_1, .., \theta_n)$ fixed over time	see appendix, inequality (C15)
Spichtig and Kawecki (2004)	$\gamma = 0$, $(\theta_1, .., \theta_n)$ fixed over time, $n = 2$	studies the effect of the number of loci
Gillespie (1973*b*)	$\gamma = 0$, $n = 1$	
Gillespie (1974)	$\gamma = 0$, $m = 1$, θ_i IID	see appendix, inequality (C16)
Gillespie (1975)	$\gamma = 0$, $n = 2$	
Gillespie (1976)	$\gamma = 0$, $n \to \infty$	
Gillespie and Langley (1976)	$\gamma = 0$, $m = 1$, $n \to \infty$, θ_i IID	
Chesson and Warner (1981); Ellner and Hairston (1994); Svardal et al. (2011)	$n = 1$	lottery model, see appendix, inequality (C14)
Chesson (1985)	$m = 1$, no temporal correlations, $n \to \infty$	patchy environment lottery (PEL) model
Comins and Noble (1985)	$\gamma = 0$, θ identically distributed	

Note: While our model covers and extends most ecological assumptions of these studies, genetic assumptions often differ. IID: identically and independently distributed.

2.6. Invasion analysis

For our analytical results we rely on the adaptive dynamics approximation (Dieckmann and Law 1996; Metz et al. 1996; Geritz et al. 1998), which is based on the assumption of rare mutations of small effect. A comprehensive account of the analytical methodology is given in appendix B. Under these assumptions, directional evolution is a sequence of substitution events leading toward trait values at which directional selection vanishes. These trait values are attractors of the trait substitution sequence. At such points, selection can be stabilizing or disruptive. In the first case, genetic variation can only be maintained at mutation-selection equilibrium, whereas in the second case genetic variation increases due to adaptive evolution. Trait values of the latter type are known as evolutionary branching points. Importantly, in the vicinity of evolutionary branching points a genetic polymorphism cannot be replaced by a single genotype. In this article, we identify the conditions for the existence of evolutionary branching points. With computer simulations we show that – in reasonably large populations – our results accurately predict the adaptive evolution of genetic polymorphism, even if the various assumptions of the adaptive dynamics approximation are violated.

We assume that at most one mutation segregates in the population at each point in time and, shortly after a new mutation has occurred, most individuals have the common "resident" trait value, x, and only few individuals have a very similar "mutant" trait value y. Then, the phenotype density in each patch is dominated by the resident phenotype (technically, $\phi_{it}(x') \approx \delta(x'-x)$, where $\delta(x'-x)$ is the Dirac delta function). Hence, the relative reproductive success of a rare mutant individual with trait value y in patch i at time t simplifies from equation (2) to

$$\rho(y, \phi_{it}, \theta_{it}) \approx \frac{r(y, \theta_{it})}{r(x, \theta_{it})} =: \rho(y, x, \theta_{it}), \tag{5}$$

where in the following we include the resident trait value x as second argument to ρ and omit the trivial phenotype density function. In other words, mutant individuals are so rare that they only compete with resident individuals during density regulation. We call the logarithm of $\rho(y, x, \theta_{it})$ "local selection coefficient" and denote it by

$$s_{it} := \ln\left(\rho(y, x, \theta_{it})\right).$$

Furthermore, we refer to its first derivative with respect to the mutant trait value, $\frac{\partial s_{it}}{\partial y}|_{y=x}$, as "local selection gradient". It measures within-patch directional selection at a given time step. The second derivative, $\frac{\partial^2 s_{it}}{\partial y^2}|_{y=x}$, called "local selection curvature" in the following, measures within-patch quadratic selection at a given time step. It can be stabilizing (< 0) or disruptive (> 0).

The relative number of mutants in the next generation in the total population is then given by equation (3), where $\rho(y, \phi_{it}, \theta_{it})$ in equations (4 a,b) is replaced with $\rho(y, x, \theta_{it})$ from equation (5). The ultimate fate of a new mutation is determined by its long term growth rate, which is called invasion fitness. More precisely, invasion fitness is the long term average change in density of individuals with the rare mutant trait value y in a population dominated by trait value x. For a

given sequence of environmental states $\{(\theta_{1,0},..,\theta_{n,0}),..,(\theta_{1,T},..,\theta_{n,T})\}$, we call $\lambda_T(y,x)$ the leading eigenvalue of the product of the population projection matrices, $\prod_{t=0}^{T}\mathsf{L}(y,x,\theta_{1t},..,\theta_{nt})$. Then, invasion fitness is given by

$$w(y,x)=\lim_{T\to\infty}\frac{1}{T}\lambda_T(y,x) \tag{6}$$

(Metz et al. 1992; Metz 2008). Our assumptions on the distribution of the $(\theta_{1t},..,\theta_{nt})$ guaranty convergence of $w(y,x)$ to a fixed value which is independent of the sequence of environmental states (c.f. appendix B).

The direction of the trait substitution sequence is given by the "global" selection gradient, $S(x)=\frac{\partial w(y,x)}{\partial y}|_{y=x}$. Directional selection vanishes for trait values x^* for which $S(x^*)=0$. Finally, a trait value x^* that is an attractor of the evolutionary dynamics and simultaneously a fitness minimum, i.e., $\frac{\partial^2 w(y,x^*)}{\partial y^2}|_{y=x^*}>0$, is an evolutionary branching point (see appendix B for details).

2.7. Simulations

We complement the analytical invasion analysis with two computational approaches. First, we use numerical iterations to calculate the branching condition. This approach implements the assumptions of adaptive dynamics, but mutations change trait values by a discrete amount and the long term success of a mutation is determined from a long but finite sequence of environmental states (cf. online supplementary D.1). Second, we employ individual-based computer simulations of the system described by equations (1)-(4). This approach considers finite populations and allows us to study different genetic systems and mutation rates and effect sizes. We consider sexually reproducing diploid genetics with the trait being determined by up to ten additive loci, each with infinitely many alleles. Mutational effect sizes are drawn from a normal distribution. Alternatively, we assume a large number of loci (50-500) with two alleles each. More details on the simulations and the commented source code can be found in online supplementary D.2 and D.5, respectively.

In the simulation study, we assume Gaussian stabilizing selection (cf. equation 1) and investigate many different distributions of environmental conditions. For the figures presented in this article, we focus on the case that the selective optima in different patches occur independently of each other and, if not mentioned otherwise, can take values 0 and 1. Furthermore, all our simulations for the case of identically distributed patches assume that both selective optima occur with equal probability (of 0.5) in all patches, while in the case of differently distributed patches we assume that selective optimum 1 occurs with probability 2/3 in half of the patches and with probability 1/3 in the other half (we always assume an even number of patches in this case). The additional parameters used in the simulation study are summarized in table 3. In the simulations, genetic variance is measured as the variance in trait values averaged over the last $8\cdot10^4$ time-steps of 10 simulations running for a total of 10^5 time-steps each.

Table 3: Standard simulation parameters

symbol	explanation	standard value
N	population size	6000
c_i, k_i	juvenile and adult carrying capacities	$1/n$
$T_{\max}$	number of time steps simulated	100000
μ_{trait}	trait mutation probability per generation	0.01
σ_μ	expected mutational effect size; effect is drawn from $N(0, \sigma_\mu^2)$	0.01
ms	bin size for mutational effects; effects are rounded to multiples of ms	0.01
k	number of loci	4
rec	recombination probability	0.01

Note: Values of other parameters are given in the respective figure legends.

3. Results

Let a_i and b_t be arbitrary functions of the environmental conditions θ_{it}. We define spatial and temporal averages as

$$\mathrm{E_S}[a] = \sum_{i=1}^{n} c_i a_i \tag{7}$$

$$\mathrm{E_T}[b] = \lim_{T\to\infty} \frac{1}{T} \sum_{t=1}^{T} b_t \tag{8}$$

Note that the a_i can explicitly depend on time (such as $a_i = \theta_{it}$), in which case also $\mathrm{E_S}[a]$ will be a function of time. Similarly, b_t can either be patch-specific (such as $b_t = \theta_{it}$) or a function of the environmental conditions across several patches. In particular, we often encounter cases such as $b_t = \sum_i c_i \theta_{it} = \mathrm{E_S}[\theta]$ in double averages $\mathrm{E_T}[\mathrm{E_S}[\theta]] = \mathrm{E_S}[\mathrm{E_T}[\theta]]$. Note that by using the self-averaging property (ergodicity) of the process that describes the environmental fluctuations, we can write equation (8) as

$$\mathrm{E_T}[b] = \int_\Omega b \cdot f(\theta_1, .., \theta_n) \mathrm{d}\theta_1 .. \mathrm{d}\theta_n. \tag{9}$$

The temporal average is thus an expectation with respect to the stationary distribution $f(\theta_1, .., \theta_n)$ of environmental states. We define variances and covariances in an analogous way, e.g., $\mathrm{Var_S}[a] = \mathrm{E_S}[a^2] - \mathrm{E_S}[a]^2$.

For brevity we introduce the following short-hand notation for the local selection gradient and the local selection curvature evaluated at a trait value x^* for which the global selection gradient (defined below equation 6) is zero:

$$\partial s_{it} := \left.\frac{\partial s_{it}}{\partial y}\right|_{y=x=x^*} \text{ and } \partial^2 s_{it} := \left.\frac{\partial^2 s_{it}}{\partial y^2}\right|_{y=x=x^*}. \tag{10}$$

In appendix B we prove that trait values x^* can be found by solving

$$\mathrm{E_T}\left[\mathrm{E_S}\left[\partial s\right]\right] = 0, \tag{11}$$

For the case of Gaussian selection, there is only one such trait value given by

$$x^* = \mathrm{E_T}[\mathrm{E_S}[\theta]] \tag{12}$$

(appendix C). Equation (11) says that global directional selection vanishes for trait values for which the spatio-temporal average of the local selection gradients equals zero. From equation (12) follows that for Gaussian selection such trait values match the spatio-temporal average selective optimum. Furthermore, such trait values x^* are evolutionary attractors if and only if

$$\mathrm{E_T}\left[\mathrm{E_S}\left[\partial^2 s\right]\right] < 0. \tag{13}$$

Thus, x^* is an attractor of the evolutionary dynamics if for this trait value the spatio-temporal average of local selection curvatures is negative, that is, if local selection is on average stabilising. Under Gaussian selection, condition (13) becomes $-1/\sigma^2 < 0$ and is always fulfilled. Note that equations (11) and (13) are independent of the dispersal probability, m, the generation overlap, γ, and of temporal and spatial correlations. The order of temporal and spatial averages can be exchanged in these formulas.

The following inequality is our main result. We show in appendix B that an evolutionary attractor x^* is an evolutionary branching point if

$$\mathrm{E_T}\left[\mathrm{Var_S}\left[\partial s\right]\right] + \gamma \mathrm{Var_T}\left[\mathrm{E_S}\left[\partial s\right]\right] + 2\frac{1-m}{m}\mathrm{Var_S}\left[\mathrm{E_T}\left[\partial s\right]\right] + \mathcal{C}\left[\partial s\right] > -\mathrm{E_T}\left[\mathrm{E_S}\left[\partial^2 s\right]\right]. \tag{14}$$

If this condition is fulfilled, there is selection for genetic polymorphism. For the case of Gaussian selection, the condition can be rewritten as

$$\sigma^2_{\mathrm{crit}} := \mathrm{E_T}\left[\mathrm{Var_S}\left[\theta\right]\right] + \gamma \mathrm{Var_T}\left[\mathrm{E_S}\left[\theta\right]\right] + 2\frac{1-m}{m}\mathrm{Var_S}\left[\mathrm{E_T}\left[\theta\right]\right] + \mathcal{C}[\theta] > \sigma^2, \tag{15}$$

where we call the left-hand side σ^2_{crit}. In both cases,

$$\mathcal{C}[a] := 2(1-\gamma)(1-m)\sum_{\Delta t=1}^{\infty}(1-(1-\gamma)m)^{\Delta t-1}\left(\mathrm{E_S}\left[\mathrm{Cov_T}\left[a_t, a_{t+\Delta t}\right]\right] - \mathrm{Cov_T}\left[\mathrm{E_S}\left[a_t\right], \mathrm{E_S}\left[a_{t+\Delta t}\right]\right]\right), \tag{16}$$

with $a = \partial s$ or θ, respectively. $\mathcal{C}[a]$ summarizes the effect of temporal autocorrelations as discussed below. Note that the covariances $\mathrm{Cov_T}[.]$ are averages over all times t, but we leave the summation index t explicit to express the dependence on the time difference Δt. Conditions (14) and (15) are readily evaluated for a given pattern of fluctuations in the environmental conditions. We compute and discuss various special cases in appendix C.3, including environmental distributions with continuous and discrete environmental states and with and without temporal and spatial correlations. In the following, we give an interpretation for each term in the branching condition.

3.1. Influence of the shape of within-patch selection

Inequalities (13) and (14) define upper and lower bounds for the average curvature of local selection. Spatio-temporal average selection must be stabilizing for the trait value x^* to be an evolutionary attractor (inequality 13). However, for evolutionary branching to occur the "diversifying" factors on the left-hand side of condition (14) have to dominate stabilizing selection. Otherwise, the trait value x^* is an evolutionary end point (sometimes called "continuously stable strategy" or CSS, Eshel 1983; inequality 14 with reversed inequality sign).

For the case of Gaussian stabilizing selection, the right-hand side of inequality (14) is $1/\sigma^2$, but the terms on the left-hand side scale with $1/\sigma^4$. Hence, stronger stabilizing selection (smaller σ^2) always promotes branching (inequality 15). Our formalism can also accommodate stabilizing selection that differs in strength among patches (but still remains constant over time). In this case, the terms in the calculation of the spatial mean and variance in condition (15) are weighted by the patch-specific factor $1/\sigma_i^2$ (see appendix C.2). Thus, patches in which selection is strong contribute relatively more to the total variance in selective optima and thus to branching.

3.2. Influence of spatio-temporal fluctuations in selection

The first two terms on the left-hand side of condition (14) describe the influence of spatial and temporal fluctuations in selection on evolutionary branching. For Gaussian selection, these fluctuations can be expressed by the fluctuations in the selective optima. In the limit of very long-lived adults ($\gamma \to 1$) both terms simply combine to the total variance over time and space and the decomposition into two parts follows the law of total variance. For $\gamma < 1$, temporal fluctuations in the spatial average selection only enter proportional to γ. Hence, such "global" temporal fluctuations only contribute to selection for genetic variation if generations overlap. This effect is known as "storage effect of generation overlap" (Chesson and Warner 1981). In contrast, expected spatial differences as described by the first term promote evolutionary branching independent of other factors.

Both terms are also affected by spatial correlations. Note that, as we assume an island model, spatial correlations are an effect across all patches and do not have a particular spatial scale. Expected spatial variation in selection is reduced by positive spatial correlations and increased by negative correlations. The opposite is true for temporal variation in the spatial mean selection gradient, because temporal fluctuations in the patches contribute more to global temporal fluctuations under positive and less under negative spatial correlations. For sufficiently small γ the first term dominates the second term so that negative spatial correlations promote branching and positive correlations impede it. Specific examples for environmental fluctuations with spatial correlation are analyzed in appendix C.3. Temporal correlations, on the other hand, do not affect the two terms in question.

3.3. Influence of spatial differentiation

The third term on the left-hand side of conditions (14) and (15), $2\frac{1-m}{m}\mathrm{Var_S}\left[\mathrm{E_T}[.]\right]$, describes an additional contribution of spatial differences in expected selection that can be interpreted as selection for local adaptation. It is zero if environmental conditions are identically distributed across patches or if all offspring disperse ($m = 1$) and increases with decreasing migration probability. In fact, if $\mathrm{Var_S}\left[\mathrm{E_T}[.]\right] \neq 0$, then for every σ^2 exists a critical value of m such that for all migrations probabilies below this critical value condition (15) is fulfilled. It is unaffected by temporal or spatial correlations. Figure 2B (solid line) shows how between-patch differences promote evolutionary branching as dispersal decreases.

3.4. Influence of temporal correlation

Temporal autocorrelations in the local selection gradients only affect the last term, $\mathcal{C}[.]$, on the left-hand side of conditions (14) and (15). This term is zero in the absence of temporal correlations. In general, positive temporal autocorrelations within patches promote branching and negative autocorrelations impede it. However, this is not true if these "local" autocorrelations are just the consequence of global temporal correlations. This can be seen from definition (16), where the temporal covariance in the spatial mean selection gradient is subtracted from the average temporal covariance within patches. Hence, local but not global temporal autocorrelations promote evolutionary branching. The reason is that local autocorrelations can lead to extended periods over which individual patches consistently experience similar environmental conditions resulting in transient phases of differentiation among patches.

The covariance terms are weighted by the factor $(1-\gamma)(1-m)(1-(1-\gamma)m)^{\Delta t-1}$, where Δt is the length of the time interval considered. This factor is always smaller than one and can be understood as follows. Similar to the effect of spatial differentiation, the diversifying effect of transient patch differences produced by positive autocorrelations requires that genotypes preferentially stay in the same patch. Hence, the effect of autocorrelations on invasion fitness is strongest for low dispersal and vanishes when all offspring disperse ($m = 1$). Generation overlap, γ, has a two-fold effect on the influence of autocorrelations. Starting from small values, increasing generation overlap first strengthens the effect of autocorrelations by increasing the probability that genetic material survives in the same patch over the considered time interval. However, as γ approaches one, the influence of temporal correlations vanishes because individuals are more likely to experience a representative sample of the distribution of environmental conditions. Finally, the just-mentioned effects of dispersal and adult death affect the genotype composition at each time-step. Hence, temporal correlations between distant time points (large Δt) enter with reduced weight.

3.5. Influence of patch number and relative patch size

The influence of the number of patches, n, can most easily be seen in the case without spatial and temporal correlations, where the branching condition can be simplified. For brevity we only give the condition for the Gaussian case here. The general result and its derivation is given in appendix C.1. In the absence of correlations, the branching condition can be expressed as

$$\frac{2-m}{m}\mathrm{Var_S}[\mathrm{E_T}[\theta]] + \left(1 - \frac{1-\gamma}{n}\right)\mathrm{E_S}\left[\mathrm{Var_T}[\theta]\right] - (1-\gamma)\mathrm{Cov_S}\left[c, \mathrm{Var_T}\left[\theta\right]\right] > \sigma^2, \qquad (17)$$

where $\mathrm{Cov_S}[.,.]$ is the spatial covariance. Here, the first term corresponds to permanent patch differences and it draws contributions from both the first and the third term in equation (15). The second term in condition (17) corresponds to the effect of within-patch fluctuations in environmental conditions and draws contributions from the first and the second term in equation (15). This term reveals that branching becomes easier with an increasing number of patches. This effect becomes weaker with increasing generation overlap. Conversely, the positive effect of generation overlap vanishes with increasing patch number. The third term on the left-hand side of condition (17) is zero if patches are equally sized or if environmental flutuations are equally strong in all patches. This term shows that a given amount of temporal fluctuation promotes branching more strongly if it is produced by relatively stronger fluctuation in the smaller patches. Conversely, it contributes less to branching if it is produced by relatively stronger fluctuations in few large patches. We plot the left-hand side of inequality (17) (σ^2_{crit}) for the case $c_i = 1/n$ as a function of the patch number and for different values of generation overlap in figure 3.

3.6. Robustness of the results

The analytical results are derived under the assumption of rare mutations of small effect and a very large population size. Then, if conditions (13) and (14) are fulfilled, there exists a trait value x^* that is an evolutionary attractor at which disruptive selection favors an increase in genetic variance and hence the evolution of adaptive genetic polymorphism. In order to study the robustness of this result with respect to violations of these assumptions, we perform extensive individual-based simulations for the case of Gaussian stabilizing selection (see online supplementary D.2 for details on the simulation study). These simulations show that populations indeed evolve towards the trait value x^* under a wide variety of genetic assumptions and population sizes. Furthermore, also our main result – the condition for adaptive genetic polymorphism – is not sensitive to the violation of the adaptive dynamics assumptions. In particular, the branching condition (inequality 14) accurately predicts an increase in genetic variance due to disruptive selection for all tested mutation rates and mutational effect sizes (figure 4, but see below for the effect of low mutation rates in small populations). Also sexual reproduction and diploid genetics with several recombining additive loci do not change this picture (figure 5). While we assume full dispersal ($m = 1$) in this figure, results also hold for other values of m (supplementary figure D2).

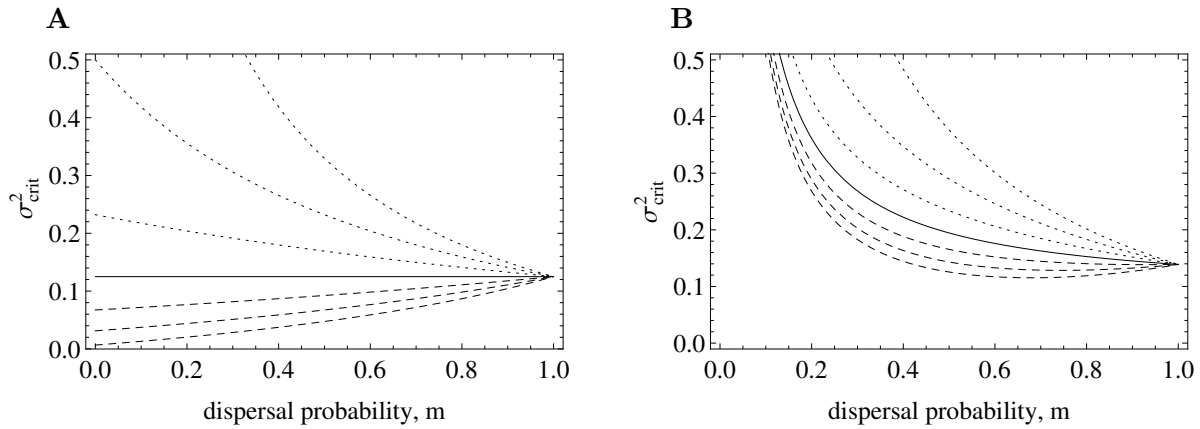

Fig. 2.— Critical strength of selection below which selection is disruptive as a function of the dispersal probability. Large values of σ^2_{crit} indicate a large scope for genetic diversification. For these plots, we assume discrete generations ($\gamma = 0$) and two patches with selective optima that fluctuate between two possible states. In both panels, solid lines give the case of no temporal correlation, dotted lines the case of positive temporal autocorrelation and dashed lines the case of negative autocorrelation. Autocorrelation increases with the distance of the dotted or dashed lines from the solid line. Details of the parametrization of autocorrelations are given in appendix C.3, where inequalities (C21) and (C22) define the curves in panel A and B. In panel A, the two alternative selective optima each occur with probability of 1/2 in both patches. Thus, the patches are identically and independently distributed. In this case, the branching condition is independent of m in the absence of temporal correlations. Positive correlations lead to a positive effect of decreased dispersal on the parameter range for branching, while negative correlations have the opposite effect. In panel B, the patches are not identically distributed, but the first selective optimum occurs in the first patch with probability 1/3 and in the second patch with probability 2/3. The opposite is true for the second selective optimum. In this case, decreasing dispersal generally has a positive effect on diversity, unless temporal autocorrelations are strongly negative.

The only factor that can introduce substantial deviations from our branching condition is population size. For small population sizes genetic variance only starts to increase for stronger selection (smaller σ^2) than predicted by our condition (14). The critical population size below which our results become inaccurate depends on the mutation parameters. In figure 6 we used a trait mutation rate of 0.01 (per locus mutation rate of $\approx 10^{-4}$) and an expected mutational effect size of 0.05. For these values we see deviations from our branching condition only for total population sizes of 100 individuals or less (figure 6A). For smaller mutation rates and effect sizes, deviations appear earlier (i.e., already for larger population sizes). This leads to the counter-intuitive conclusion that the branching condition becomes increasingly robust for small population size as the adaptive dynamics assumptions of rare mutations and small mutational effects are violated. The reason for this behavior is that in small populations random fluctuations in selection can easily lead to a loss

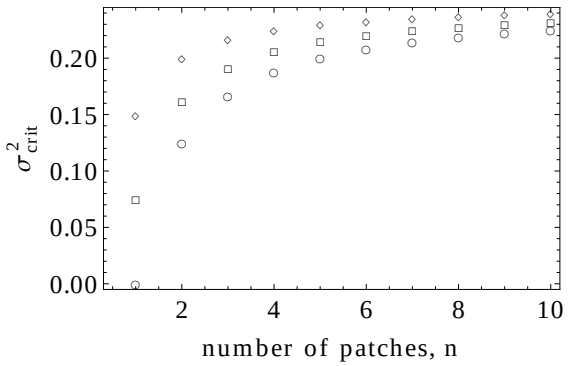

Fig. 3.— Critical strength of selection below which selection is disruptive as a function of the number of patches as given by condition (17). Results shown for generation overlap $\gamma = 0$ (circles), $\gamma = 0.3$ (squares), $\gamma = 0.6$ (diamonds), $m = 1$, and $c_i = 1/n$. Increasing the patch-number facilitates diversification (cf. second term on the left-hand side of condition 17).

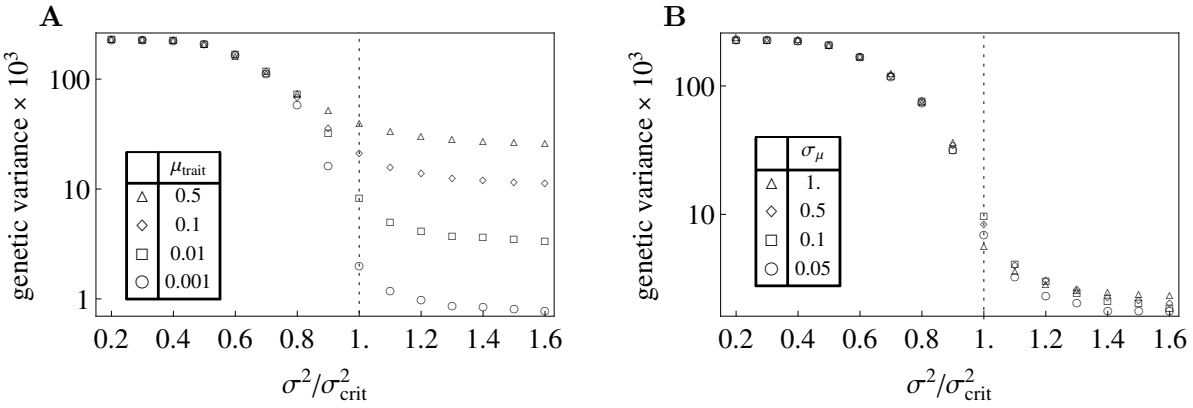

Fig. 4.— Long-term average genetic variance (on log-scale) measured from individual based simulations as a function of the strength of Gaussian stabilizing selection for different (A) mutation rates and (B) expected mutational effect sizes. Selective optima fluctuate independently across five patches. Spatial differences in expected selection and spatial and temporal correlations are absent. The dotted vertical line indicates the analytically expected branching point $\sigma^2/\sigma^2_{\text{crit}} = 1$ (cf. inequality 15). In all cases, the analytical condition for evolutionary branching coincides with the observed incarease in genetic variance in individual based simulations. Note that in panel A the amount of genetic variation is determined by mutation selection balance when the branching condition is not fulfilled (right of the dashed line) but becomes independent of mutation rate when the branching condition is fulfilled (left of the dashed line). Parameters: $\gamma = 0.5$, $m = 1$; other parameters as in table 3.

of genetic variation, which is necessary for disruptive selection to act upon. Importantly, this effect is almost entirely due to random fluctuations in the expected size of the mutant sub-population

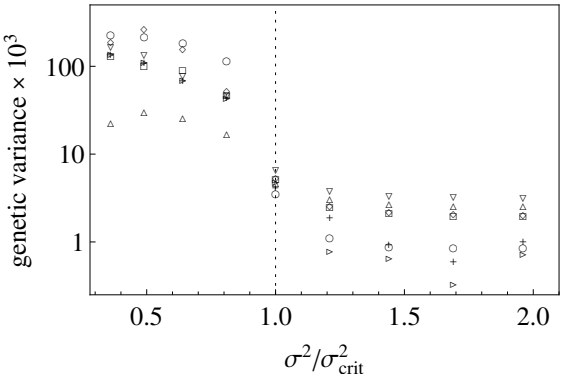

symbol	n	γ	ploidy	loci	rec
○	5	0.5	haploid	1	0
□	5	0	diploid	3	0.3
◇	8	0	diploid	3	0.3
△	2	0	diploid	10	0.05
▽	5	0	diploid	10	0.05
+	5	0.5	diploid	50	0.05
▷	5	0.5	diploid	500	0.05

Fig. 5.— Long-term average genetic variance (on log-scale) measured from individual based simulations as a function of the strength of Gaussian stabilizing selection for the case of full dispersal ($m = 1$) for various ecological parameters and genetic architectures (see table). The dotted vertical line indicates the analytically expected branching point $\sigma^2/\sigma^2_{\text{crit}} = 1$ (cf. inequality 15). Genetic variance increases substantially if the branching condition is fulfilled. This holds true for all examined combinations of ecological and genetic scenarios as detailed in the table. Selective optima in the patches are identically and independently distributed. Parameters: $\mu_{\text{trait}} = 0.01$; other parameters as given to the right of the plot or in table 3.

produced by environmental stochasticity and not due to classic genetic drift (i.e., variance among replicates for a fixed sequence of environments). Indeed, the effect remains unchanged if the random sampling step in recruitment is removed and the number of offspring of each individual is equal its expectation (rounded to integer). Figures D3 and D4 show the accuracy of our results for other mutational and ecological parameters. In figure 6B we use a constant total population size and test the influence of local population sizes by varying the number of patches. We only get substantial deviations from the analytical prediction if the patches are very small (five or ten individuals per patch). Hence, while a large number of patches promotes evolutionary branching (cf. inequality 17), extremely small patch sizes are detrimental to adaptive genetic polymorphism.

3.7. Genetic structure of the polymorphism

In the previous section we have shown that, in reasonably large populations, increased levels of genetic variation evolve if the branching condition is fulfilled. Here we examine the structure of the resulting genetic polymorphism.

In sufficiently large populations of clonally reproducing organisms and in the absence of environmental stochasticity, populations split at a branching point into two discrete sub-populations that evolve away from each other in phenotype space while negative frequency dependence protects them from extinction. If there are more than two possible selective optima and if these are sufficiently distant from each other relative to the strength of selection, then the sub-populations can

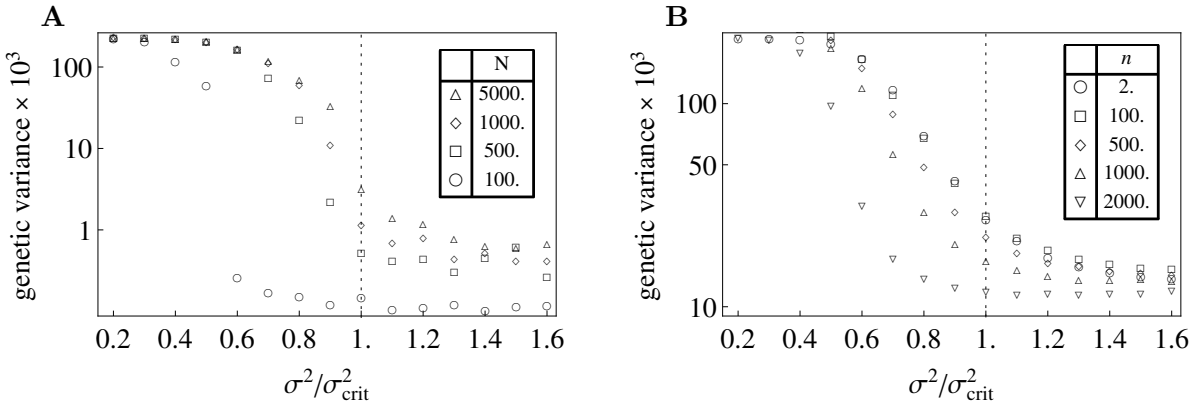

Fig. 6.— Long-term average genetic variance in a population (on log-scale) from individual-based simulations as a function of the strength of Gaussian stabilizing selection for identically and independently distributed selective optima across patches (cf. figure D2A). In panel A the total population size (N) is varied for a constant number of $n = 5$ patches. In populations of 100 individuals or less, the increase in genetic variance only happens for smaller values of σ^2 (stronger selection) than predicted by the branching condition. In panel (B) the number of patches (and hence the local population size) is varied for a constant total population size of $N = 10000$. It shows that only for very small patch size ($n > 1000$, less than 10 individuals per patch) the increase in genetic variance is substantially delayed as compared to the analytical predictions. Parameter values: $\gamma = 0.5$, $m = 1$, $\sigma_\mu = 0.05$; other parameters as in table 3.

split again until a polymorphic equilibrium is reached at which each type experiences stabilizing selection. Such a scenario is described in more detail in Svardal et al. (2011, figure 6).

However, in populations of biologically realistic size the genetic polymorphism can look very different, mainly depending on two factors: (1) the strength of demographic fluctuations in the sub-populations characterized by different trait values, due to environmental stochasticity and drift, and (2) the genetic architecture of the trait.

Environmental stochastiticy can be understood as the deviation of the growth rate of a mutant sub-population over a finite time interval from the invasion fitness (equation 6). Such excursions of the short-term growth rate from its long-term average are caused by the random fluctuation in the environmental conditions. In our model, the strength of environmental stochasticity is increased by (i) a large temporal variance in environmental conditions within each patch, (ii) a small number of patches, (iii) positive spatial and temporal correlations, (iv) a small spatial variance in expected environmental conditions, (v) small generation overlap (for the effect of generation overlap, see Svardal et al. 2011, figure 7), and (vi) strong stabilizing selection (small σ^2).

Figure 7 shows the effect of environmental stochasticity by varying the number of patches. For eight patches (figure 7, bottom panel), environmental stochasticity is sufficiently weak so that we observe the above-mentioned stable polymorphism. For the case of five patches (figure 7, middle

panel), environmental stochasticity is stronger and a series of environmental states unfavorable to one sub-population can lead to its extinction. The remaining sub-population then evolves back to the branching point where it subsequently splits again to restore the genetic polymorphism. With only two patches (figure 7, top panel), environmental stochasticity is so strong that extinction of sub-populations happens very frequently and no clear split of the population into discrete branches is visible (figure 7, top panel). However, even in such a regime there is a detectable increase in genetic variance when the branching condition is fulfilled (except for the cases of very small population size mentioned above). Note that the precise number of patches, for which each of these regimes can be observed, depends on the other factors discussed above.

Interestingly, population size – while being important for the general accuracy of our branching condition – only plays a minor role for the stability of the genetic polymorphism. Its influence on the stability of polymorphism seems to be logarithmic. Finally, while strong selection increases the effect of environmental stochasticity and therefore favors the extinction of subpopulations it is necessary that selection is sufficiently strong for polymorphism to emerge in the first place. This two-fold effect can be seen in figures 5 (tip-up triangles) and D2, where for some parameter combinations genetic variance decreases for very small σ^2.

The second factor that influences the structure of the genetic polymorphism is the genetic basis of the trait. While clonal populations can split into discrete phenotypic clusters that each evolve towards a peak in the fitness landscape, this is not possible for sexual populations because mating between individuals from two different clusters results in intermediate phenotypes (Dieckmann and Doebeli 1999; Kisdi and Geritz 1999). In figure 5 we show by means of individual-based simulations that also sexually reproducing diploid populations evolve increased levels of genetic variance for a wide range of ecological and genetic assumptions. This is in particular true for various multi-locus cases. The structure of the genetic polymorphism depends on the ploidy, the number of loci, and the recombination rate. The patterns observed range from one intermediate phenotype (heterozygote) between two diverging branches for a single diploid locus, to a cloud of phenotypes for many recombining loci. Figure 8 shows an example of a simulation run for a diploid population in which the trait is determined by four additive and strongly recombining loci. Disruptive selection initially leads to evolutionary branching at all loci resulting in a cloud of phenotypes. Only after the dimorphism at one locus is lost, discrete phenotypic clusters become visible. The long-term expectation is that the genetic polymorphism becomes concentrated at a single locus, while all other loci become monomorphic (Kopp and Hermisson 2006; van Doorn and Dieckmann 2006; Yeaman and Whitlock 2011), because this minimizes the amount of maladapted intermediate phenotypes.

Another effect of sexual reproduction and a multi-locus genetic architecture is that it counteracts the extinction of alleles in the polymorphism due to environmental stochasticity because extreme types that have disappeared during adverse conditions can be restored from intermediate types by recombination.

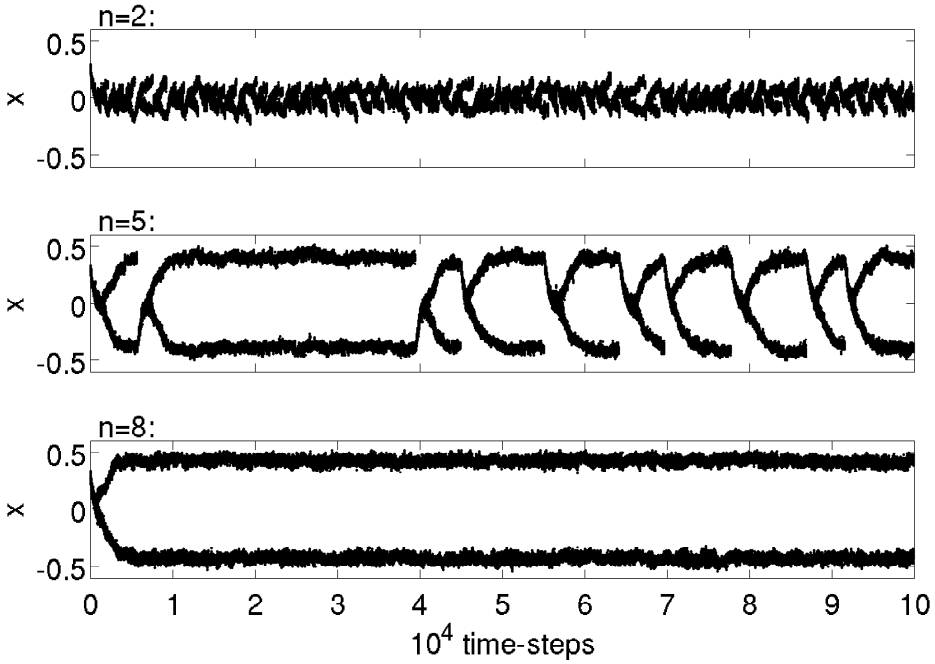

Fig. 7.— Population trait values over time from individual-based simulations for three different patch numbers at a constant total population size of $N = 4000$. Selective optima are identically and independently distributed across patches and we assume a single haploid locus. Note that the two alternative selective optima are at -0.5 and 0.5 instead of 0 and 1. For a small number of patches the genetic dimorphism is frequently lost, and with increasing n the dimorphism becomes increasingly stable. Parameter values: $\mu_{\text{trait}} = 0.001$, $\gamma = 0$, $m = 1$, $\sigma^2 = 0.09$; other parameters as given in table 3.

4. Discussion

When does temporally and spatially fluctuating selection favor the evolution and maintenance of genetic diversity in a population? We investigate this question for a generalized island model (Wright 1943) that we combine with the simple age structure of the lottery model (Chesson and Warner 1981) so that generations can overlap. Our model is characterized by the following features. The population decomposes into patches of locally competing individuals from which a certain fraction of juveniles disperses each generation over the whole population. The population is thus subdivided, but there is no isolation by distance. Environmental conditions can fluctuate over time, either independently in different patches or with arbitrary spatial and temporal correlations. The environment exerts selection on a quantitative trait. Selection acts only on a single, short-lived life stage (e.g. juveniles), while a long lived stage survives from one reproductive season to the next with a constant probability, independent of trait and locality. The total reproductive output of

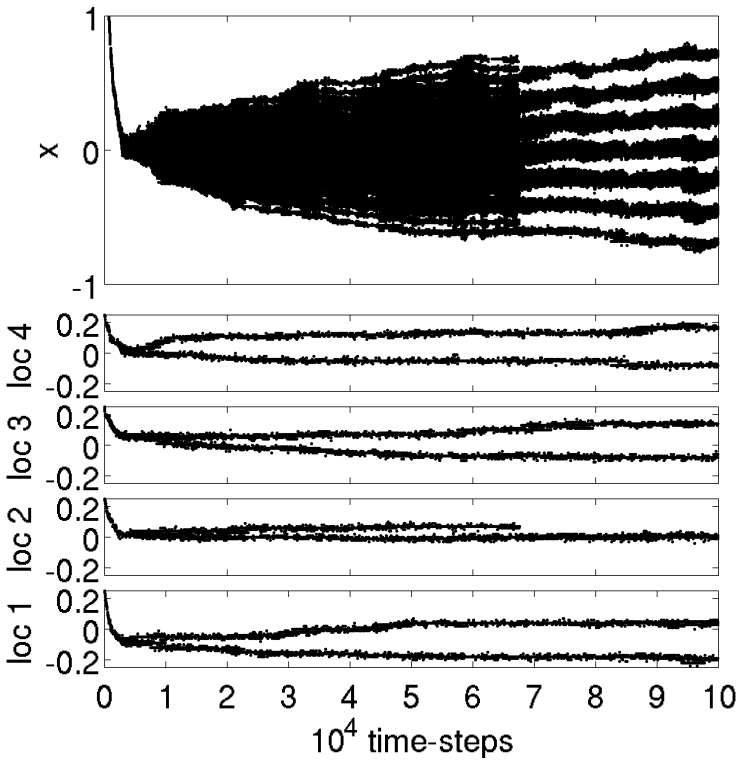

Fig. 8.— Population trait values (top panel) and allelic values at four diploid additive loci (lower panels) over time from individual based simulations. The two alternative selective optima are at ± 1. Branching initially happens at all four loci. At the phenotypic level this results in a cloud of different phenotypes. After the polymorphism at locus 2 goes extinct around time-step 70000, discrete phenotypic clusters become visible. Parameter values: $N = 4000$, $n = 4$, $m = 1$, $\gamma = 0.1$, $rec = 0.3$, $\mu_{\text{trait}} = 4 \times 10^{-4}$; other parameters as in table 3.

each patch is constant (soft selection).

Our ecological model includes several standard models of ecology and population genetics as special cases (see table 2). In contrast, our genetic assumptions differ from most previous models listed in table 2. While the latter usually focus on two alleles or two species, we consider a quantitative trait and we ask under which conditions selection on the trait turns disruptive, so that genetic polymorphism is selected for. Technically, we do this by using the adaptive dynamics approximation (Metz et al. 1996; Geritz et al. 1998) to identify conditions for the existence of evolutionary branching points. These are trait values that are on the one hand attractors of the evolutionary dynamics, but at which, once the majority of the population is sufficiently close to them, selection turns disruptive. Evolutionary branching points are the signature of negative frequency-dependent selection due to intraspecific competition. We obtain a very general condition for evolutionary branching and thus for the adaptive evolution and maintenance of genetic diversity

in temporally and spatially heterogeneous environments (equations 11-15). This is our main result.

4.1. Factors promoting adaptive diversification

We can distinguish four main factors that promote adaptive genetic polymorphism, which each capture an aspect of the temporal and spatial heterogeneity. A detailed quantitative analysis is provided in the results section and the supplements. A more intuitive interpretation of the results can be given in terms of ecological niches.

First, ecological niches are created by spatial differences in selection. On the one hand, such differences can arise from spatial differences in the expected environmental conditions ("permanent niches"). On the other hand, temporal fluctuations within patches can lead to spatial differences in selection even in the absence of permanent differences ("fluctuating niches"). Permanent niches enter our condition for genetic diversification via two terms. The first contribution (first term in inequality 15) is independent of dispersal. Note, that this is the only factor creating ecological niches in the classical Levene model with no fluctuations within patches and full migration (Levene 1953); our results reproduce previous findings for the Levene model by Geritz et al. (1998) (appendix C.3.2). The second contribution to permanent niches (third term in inequality 15), only exists under restricted dispersal ($m < 1$) and becomes increasingly important as dispersal decreases by allowing for local adaptation (Deakin 1966, 1968; Gillespie 1975; Snyder and Chesson 2003). In spatially heterogeneous environments, rare types can accumulate in patches with favorable environmental conditions leading to a positive fitness-density covariance for rare types and thus favoring coexistence (cf. Chesson 2000*a*). In the absence of spatial correlations, both contributions to permanent niches can be combined into a single term (first term in condition 17). Fluctuating niches are also captured by the first term in condition (15) and, hence, their importance is independent of the strength of dispersal as long as it is positive. Generally, fluctuating niches are less efficient in promoting adaptive differentiation than permanent niches, but their contribution increases with an increasing number of patches and with increasing negative spatial correlations across patches, while positive correlations have the opposite effect. The effect of independent temporal fluctuations on genetic polymorphism was already observed in population genetic models by Gillespie (1974; 1975; 1976; Gillespie and Langley 1976) and ecological models by Chesson (1985) and Comins and Noble (1985). Chesson (1985) found local temporal fluctuations as effective in promoting polymorphism as permanent spatial niches. However, from our results it is clear that Chesson's finding only holds under full dispersal and for sufficiently many patches (see equation 17).

Second, if generations overlap, temporal fluctuations can create ecological niches even in the absence of spatial variation (second term in equation 15). This phenomenon, known as "storage effect of generation overlap" (Chesson 1984) or "time-dispersal" (Comins and Noble 1985), can be understood as the appearance of ecological niches in the same patch over the life time of an individual (which increases with increasing generation overlap). The storage-effect was first described in the lottery model (Chesson and Warner 1981). We find the branching condition for this model

as derived by Ellner and Hairston (1994, equation 9) to be a special case of ours (appendix C.3.1).

Third, under limited dispersal, positive temporal correlations in environmental conditions stabilize ecological niches and therefore increase the scope for genetic polymorphism while negative temporal correlations reduce it (fourth term in equation 15). Intuitively, if dispersal is restricted, and if there is a higher than average chance that the local environment stays similar (positive temporal correlation), rare types can accumulate in patches where they have higher growth rates. In contrast, if individuals stay in their patch of origin but the local environment is likely to change, specialized phenotypes are selected against. To our knowledge, this effect has not been described in the literature on the maintenance of polymorphism. However, it is known that positive temporal autocorrelations in the growth rates promote species persistence in a metapopulation (e.g. Schreiber 2010). This is a closely related phenomenon since adaptive diversification depends on the persistence of rare mutant invaders.

Fourth, ecological niches created by the above-mentioned factors only promote genetic diversity if "specialist" genotypes that evolve adaptation to these niches have an advantage over "generalist" genotypes that equally exploit all niches. In other words, for genetic diversification to be favored, there have to be sufficiently strong trade-offs for the performance in different niches. In our model, stronger trade-offs are reflected by increasing average within-patch stabilizing selection. Hence, increasing the strength of stabilizing local selection promotes population-level disruptive selection for genetic polymorphism.

4.2. Generality of the results

Our analytical conditions are derived under the assumption of large populations and rare mutations of small effect. However, we show with individual-based simulations that the branching condition reliably predicts the emergence and maintenance of genetic variance for a wide range of genetic and ecological details (figures 4, 5 and D2). Sexual reproduction, if anything, further facilitates the maintenance of increased levels of genetic diversity due to its capacity to restore lost phenotypes by recombination.

We only see substantial deviations from our analytical result in small populations with low mutation rates (i.e., low new mutational input). The reason is that in such a situation demographic fluctuations quickly remove the genetic variation introduced by mutation. Hence, disruptive selection looses its target. Such an effect has been described for the action of demographic stochasticity ("sampling drift", cf. Ajar 2003; Claessen et al. 2007; Wakano and Iwasa 2013). However, in our case it is rather caused by fluctuations in the expected number of mutants due to environmental stochasticity (for a similar result in a different model, see Johansson and Ripa 2006). This can be seen, because the effect is unchanged if random sampling is removed during density regulation, whereas it vanishes in the absence of temporal fluctuations. For biologically reasonable mutation rates, such deviations only become important for total population sizes of below 100-1000 individu-

als (figures 6 and D3). Furthermore, very small local population sizes (less than 10 individuals per patch) lead to similar deviations from our branching condition. Stable coexistence in a protected polymorphism is based on the selective advantage of rare genotypes. However, if patches are very small, already a small number of copies of a genotype corresponds to an appreciable frequency and hence the potential for negative frequency-dependent selection is weakened. In the extreme case of only two individuals per patch, there is no negative frequency dependence and evolutionary branching is impossible (see online figure D3). The effect of small patch sizes has previously been described in competition models (Day 2001; Ajar 2003).

Individual-based simulations further reveal that the genetic structure of the evolving polymorphism depends on two factors. First, strong environmental stochasticity can lead to the extinction of genotypes in a polymorphism and therefore to a repeated pattern of branching and extinction events (cf. Claessen et al. 2007; Johansson et al. 2010). Second, the polymorphism pattern depends on the genetic architecture of the trait. Under clonal reproduction we readily obtain discrete phenotype clusters. For sexual reproduction, in contrast, diverging alleles at different loci recombine and a connected cloud of phenotypes can emerge. In the long run, however, several mechanisms can evolve in sexual populations under disruptive selection that prevent the production of intermediate phenotypes (Rueffler et al. 2006). These include a single major effect locus (Kopp and Hermisson 2006; van Doorn and Dieckmann 2006), dominance modifiers (Van Dooren 1999; Peischl and Schneider 2010), and assortative mating (Dieckmann and Doebeli 1999; Pennings et al. 2008). Finally, we note that, while our results are formulated in terms of genetic diversity within a species, they can also inform us about the outcome of an immigration event where an already reproductively isolated species is added to a species that has evolved sufficiently close to a singular point. If the singular point is a branching point and if the immigrating species is sufficiently similar to the resident species, then the two species are able to coexist and will subsequently undergo character displacement.

Previous studies on polymorphism in heterogeneous environments can broadly be classified in two categories: Studies following the "classic" approach of deriving conditions for the stable coexistence of a given set of alleles or species in a protected polymorphism and studies that investigate evolutionary branching in a quantiative trait. As discussed above, our findings are in qualitative agreement with classic results on coexistence in variable envrionments (e.g. Levene 1953; Dempster 1955; Deakin 1966, 1968; Christiansen 1974; Gillespie 1973*b*, 1974, 1975; Karlin 1982; Chesson and Warner 1981; Chesson 1985; Comins and Noble 1985), but some differences arise due to the difference in genetic assumptions. In particular, our condition can be both more stringent or less restrictive than the condition for stable coexistence of two fixed alleles. On the one hand, our condition is more restrictive since it requires long-term evolutionary stability in the sense that the polymorphism cannot be replaced by a generalist with intermediate phenotype (cf. Kisdi and Geritz 1999; Spichtig and Kawecki 2004). Indeed, as soon as any temporal or spatial heterogeneity in selection exists (left-hand side of inequality 14 non-zero) coexistence of suitable pairs of alleles is possible (appendix C.4; Kisdi and Geritz 1999). However, such polymorphism will only persist on

an evolutionary time scale if intermediate phenotypes are inferior (conditions 13 and 14 fulfilled). On the other hand, our branching condition can be less restrictive, because it measures disruptive selection on the quantitative trait only locally, i.e., for phenotypically similar genotypes. This local condition does not necessarily imply coexistence of alternative phenotypes that are far away in trait space. This leads to the main discrepancy between our results and earlier studies: If the patches are identically distributed, our local condition for genetic polymorphism is independent of the dispersal probability. In contrast, Gillespie (1975) and Comins and Noble (1985) found for the same scenario that the condition for protected polymorphism of discrete alleles becomes more restrictive with decreasing dispersal. Numerical calculations (appendix D.1) and individual based simulations (figure D2B) show how these results can be reconciled: The local condition for the existence of disruptive selection is independent of the dispersal probability, but the maximal phenotypic distance between genotypes that can coexist in a polymorphism decreases with decreasing dispersal. Hence, while the onset of selection for genetic polymorphism is independent of the dispersal probability, the amount of genetic variance that can evolve after branching decreases with reduced dispersal (figure D2B).

Previous models investigating evolutionary branching in subdivided populations either assume two patches connected by migration (e.g. Meszéna et al. 1997; Day 2000; Kisdi 2002) or many patches connected through a common dispersal pool (e.g. Parvinen and Egas 2004; Nurmi and Parvinen 2008). None of these models considers the combination of spatially and temporally heterogeneous environments and overlapping generations. Although these models also assume within-patch density regulation, the population size is not fixed but can change as a result of the evolutionary dynamics. The prize for relaxing the assumption of fixed within-patch densities is that the condition for branching can generally not be derived analytically. Nevertheless, qualitatively these models are in agreement with our branching condition in the sense that limited migration and pronounced patch differences favor the existence of evolutionary branching points. However, while in our model under Gaussian selection the generalist strategy is always an attractor of the evolutionary dynamics, in the references cited above it becomes evolutionarily repelling for very large patch differences in combination with low migration rate. A cursory analysis shows that this qualitative difference is indeed due to the trait dependence of local population densities.

The life cycle in our model can be found in a wide range of organisms. In this article, we equated the long-lived life stage with adult individuals. Obvious examples are perennial plants, corals, some fungi or vertebrates. Alternatively, the long-lived stage can be a resting stage (Chesson 1984; Ellner and Hairston 1994) such as a seed bank in plants, resting eggs in crustaceans, fungal spores or bacterial endospores. In such cases, the parameter $1-\gamma$ gives the rate of recruitment from the resting stage into the reproducing population. Furthermore, while we assumed that selection acts upon juvenile viability (before density regulation), our results are equally valid if selection acts upon an adult trait contributing to fertility. We briefly discuss the case of selection on recruitment probability in appendix A.2. An important aspect of our result for empirical applications is that the condition for adaptive diversification does not depend on any details in the distribution of

environmental conditions beyond its mean values and (co-)variances. Given a sufficiently long time series of measured data, these quantities can be estimated in natural systems.

4.3. Limitations and Extensions

The model presented in this article has several limitations. First, we assume that dispersal is global, that is, that there is no isolation by distance. Comins and Noble (1985) studied the case that dispersal is limited to six neighboring patches and found that local dispersal has little effect on the overall conclusions. If patches are equally sized and their environmental conditions are identically distributed, then our results equally apply to a stepping stone dispersal model (results not shown). Furthermore, if selection only varies spatially, it has been shown by Débarre and Gandon (2010) that isolation by distance has no qualitative effect on branching compared to an island model. Second, we assume that offspring are regulated locally within the patches (soft selection) to a constant density before dispersal. This assumption is most obviously fulfilled in systems with competition for space. However, in any biological system there will be traits that do not (or only slightly) influence the carrying capacity and these traits can still be under selection. Models with local density regulation but trait dependent equilibrium population densities have been discussed in the previous paragraph. In the case of global density regulation, genetic polymorphism is generally not adaptively maintained (Dempster 1955). In nature, density regulation is often due to a mixture of local and global factors. Débarre and Gandon (2011) showed that, as long as there is some local density regulation component, there is scope for the evolution of genetic polymorphism, but the condition will be more stringent. Third, we assume that the fraction of juvenile immigrants into a patch is proportional to the juvenile carrying capacity of that patch (conservative migration). This assumption is necessary for analytical tractability and has the consequence that our results are independent of the adult carrying capacities. Hence, fluctuations in adult population sizes do not change our conclusions. Fourth, in our model there is no frequency-dependent competition within patches. Frequency dependence comes from the fluctuations in selection over time and across patches in combination with soft selection. Resource competition with frequency dependence within patches has been analyzed in the context of spatially structured populations by Day (2000, 2001), Ajar (2003) and Nilsson and Ripa (2010*a*), and for the future it would be interesting to combine both effects in a single study. Fifth, we assume the dispersal probability, m, to be a parameter rather than an evolvable trait. Several models that treat the joint evolution of habitat specialization and dispersal propensity suggest that polymorphic coexistence is further facilitated by the evolution of different dispersal strategies (Kisdi 2002; Nurmi and Parvinen 2011) and even more so under the evolution of habitat choice (Ravigné et al. 2009). Finally, in our study, mutations and finite population size are only treated in simulations. There is a number of theoretical studies that use diffusion approximations to derive allele frequencies under mutation-selection-drift balance in similar ecological scenarios (Wright 1948; Kimura 1954, 1955; Gillespie 1973*a*; Karlin and Levikson 1974; Taylor 2008). Especially Taylor (2008) gives a comprehensive account of the balance of these forces under fluctuating selection.

In this study, we focused on the evolution of genetic variation in response to negative frequency-dependent disruptive selection. In principle, however, any mechanism increasing phenotypic variation is favored under this condition (reviewed in Rueffler et al. 2006). Adaptive genotype-environment interaction (phenotypic plasticity, West-Eberhard 2003; Via and Lande 1987; Gillespie and Turelli 1989), sexual dimorphism (Bolnick et al. 2003; van Doorn et al. 2004) and random phenotype determination (Leimar 2005; Svardal et al. 2011) are well studied alternatives. In cases where more than one mechanism exists that can increase phenotypic variation, it is interesting to ask which of these is more likely to evolve. The odds for the evolution of genetic polymorphism versus the evolution of randomly determined alternative phenotypes have been compared by Leimar (2005) and Svardal et al. (2011). Svardal et al. (2011) show that under temporal fluctuations in a single panmictic population ($n = 1$, lottery model) genetic polymorphism and random phenotype determination are equally favored only in the limit of infinite generation overlap ($\gamma \to 1$). For $\gamma < 1$, random phenotype determination is the favored evolutionary response to disruptive selection, if it can evolve without constraints, because it also serves as a "bet-hedging" strategy under temporally fluctuating selection. For the current model, we speculate the following. For disruptive selection due to spatial differences in the expected environmental conditions ("permanent niches") and full dispersal, genetic polymorphism and random phenotype determination are equally favored. However, as dispersal decreases, genetic polymorphism gains an advantage over random phenotype determination because the genotype serves as cue for future environmental conditions resulting in local adaptation (Leimar 2008). This effect is amplified by positive temporal correlations. On the other hand, under temporally fluctuating selection, and more so with negative temporal correlations, random phenotype determination is favored, because then a benefit due to bet-hedging arises and the genotype becomes a misleading cue for future environments. A comparison of the advantage of genetic phenotype determination relative to adaptive phenotypic plasticity in a spatially heterogeneous environment was performed by Leimar et al. (2006). These authors show that – in line with previous research – the benefit of plasticity strongly depends on the reliability of environmental cues. Furthermore, under restricted migration and strong local selection genetic polymorphism can be favored more strongly because the genotype can be an even better predictor of the coming selective environment. Applying this rationale to our model, we predict that negative temporal autocorrelations in the environmental conditions disfavor genetic polymorphism relative to plasticity because the genotype loses its value as a predictor for future environmental conditions.

Varying selective pressures and their implications for genetic diversity within species and for species diversity have always been major topics in ecology and evolution. Empirical examples for genetic polymorphism under heterogeneous selection include melanism in moth (Cook 2003) and mice (Nachman et al. 2003; Vignieri et al. 2010), pesticide resistance in insects (McKenzie 1996) and rats (Pelz et al. 2005), and pathogen resistance in animals (e.g. MHC polymorphism, Spurgin and Richardson 2010) and plants (e.g. R-gene polymorphism, Bergelson et al. 2001). For a review see Hedrick (2006). Furthermore, empirical studies show that genetic variance is positively correlated with environmental heterogeneity both in natural (Nevo 1978) and lab conditions (Mackay 1981; Kassen 2002) and that adaptive traits show substantial genetic variation (Houle 1992). Byers (2005)

argued that no comprehensive models exist that give the potential of heterogeneous environments to maintain genetic variation in traits of adaptive significance. Our present study should be seen as a step in the lasting endeavor to fill this gap.

5. Acknowledgements

We thank Peter Chesson, Troy Day, Hans Metz, Reinhard Bürger and the reviewers for comments that helped improving the manuscript. The individual based computer simulations presented have been achieved using the Vienna Scientific Cluster (VSC). The authors gratefully acknowledge funding from the Vienna Science and Technology Fund (WWTF) through grants MA06-01 and MA07-015.

A. Appendix: Ecological model

A.1. Population projection matrix

Each generation, a fraction $(1-\gamma)$ of the adults in each patch is replaced by juveniles. Hence, we have

$$\phi_{i,t+1}(y) = \gamma\phi_{it}(y) + (1-\gamma)\phi^o_{it}(y), \tag{A1}$$

where $\phi^o_{it}(y)$ is the frequency of individuals with trait value y among offspring individuals in patch i at time t. To calculate $\phi^o_{it}(y)$, we make two assumptions. First, local and dispersing juveniles have the same chance for recruitment into the adult population and, second, dispersing juveniles arrive in patch i with a probability given by the relative juvenile carrying capacity of this patch, c_i. Then, we have

$$\phi^o_{it}(y) = \frac{(1-m)c_i\phi_{it}(y)\rho(y,\phi_{it},\theta_{it}) + mc_i\sum_j c_j\phi_{jt}(y)\rho(y,\phi_{jt},\theta_{jt})}{(1-m)c_i\int_{-\infty}^{\infty}\phi_{it}(x)\rho(x,\phi_{it},\theta_{it})\mathrm{d}x + mc_i\sum_j c_j\int_{-\infty}^{\infty}\phi_{jt}(x)\rho(x,\phi_{jt},\theta_{jt})\mathrm{d}x}, \tag{A2}$$

where the numerator describes the frequency of offspring with phenotype y and the denominator normalizes with all offspring that compete for establishment in patch i. The terms proportional to $(1-m)$ correspond to non-dispersing individuals, the terms proportional to m correspond to individuals that disperse into patch i. Noting that $\int_{-\infty}^{\infty}\phi_{.t}(x)\rho(x,\phi_{.t},\theta_{.t})\mathrm{d}x = 1$ and that $\sum_j c_j = 1$, the denominator of (A2) simplifies to c_i. This means that the relative proportions of local offspring and immigrants among the newly recruited individuals in each patch are $1-m$ and m, respectively, and we obtain

$$\phi^o_{it}(y) = (1-m)\phi_{it}(y)\rho(y,\phi_{it},\theta_{it}) + m\sum_j c_j\phi_{jt}(y)\rho(y,\phi_{jt},\theta_{jt}). \tag{A3}$$

Plugging this into equation (A1) we obtain the elements of the population projection matrix given in equation (4).

A.2. Selection on recruitment probability

Here we treat the case that phenotype-dependent selection happens on the recruitment probability into the adult population. In particular, all adult individuals initially produce an equal amount of offspring, $r(y,\theta_{it}) = r$, but offspring have trait-dependent recruitment performances $b(y,\theta_{it})$ into the adult population. For simplicity we assume for this part that all offspring disperse $(m = 1)$. Then, equation (A1) still holds, but $\phi^o_{it}(y)$ is now given by

$$\phi^o_{it}(y) = \sum_j c_j\phi_{jt}(y)\frac{b(y,\theta_{jt})}{\int_{-\infty}^{\infty}\mathrm{E_S}[\phi_t(x)]b(x,\theta_{jt})\mathrm{d}x} \tag{A4}$$

where $\mathrm{E_S}[\phi_t(x)] = \sum_k c_k\phi_{kt}(x)$ is the frequency of individuals with trait value x in the dispersal pool. Note that l_{ij} takes the same form as in equation (4a), with ρ replaced by the fraction

in equation (A4). Hence, under full dispersal, selection on juvenile survival and recruitment are similar, except that in the second case there is a global mix of competitors. For $m < 1$ the denominator in equation (A4) becomes more complicated and depends on m.

B. Appendix: Analytical methods – evolutionary invasion analysis

Following the adaptive dynamics approach (Dieckmann and Law 1996; Metz et al. 1996; Geritz et al. 1998), we assume that mutations change a trait value x by a small amount to $y = x + \delta x$. Mutations are rare enough so that the previous mutation has either gone to fixation or disappeared from the population before a new mutation arises. For each new mutant it is then determined whether it can invade and replace the resident type and thus become the new resident itself. The fundamental tool to predict this dynamics is the invasion fitness $w(y, x)$, which is defined as the long-term average per capita exponential growth rate of an infinitesimally small mutant sub-population with trait value y in the resident population with trait value x (Metz et al. 1992; Metz 2008).

In sufficiently large populations, a mutant has a positive probability to invade if $w(y, x) > 0$ and is doomed to extinction if $w(y, x) < 0$. Furthermore, if mutations have a sufficiently small phenotypic effect, successful invaders will go to fixation and replace the resident (Geritz 2005). The evolutionary dynamics is then given by a series of mutation-substitution events. The direction of the evolutionary dynamics is predicted by the selection gradient,

$$S(x) = \left.\frac{\partial w(y,x)}{\partial y}\right|_{y=x}. \tag{B1}$$

Points x^* where directional selective forces vanish, i.e., where $S(x^*) = 0$, are called evolutionarily singular points (Metz et al. 1996; Geritz et al. 1998). Singular points can be classified according to whether they are an attractor of the evolutionary dynamics and whether they are invadable.

A singular point x^* is an attractor of the evolutionary dynamics if

$$\left.\frac{\partial S(x)}{\partial x}\right|_{x=x^*} < 0 \tag{B2}$$

and repelling when the inequality is reversed (Eshel 1983; Abrams et al. 1993; Metz et al. 1996; Geritz et al. 1998). In appendix C we show that in our model in the case of Gaussian selection a unique singular point exists that is always an attractor.

Since by definition the selection gradient at a singular point equals zero, the fitness landscape locally around a singular point is described by the second partial derivative of invasion fitness with respect to the mutant trait. The singular point is a local fitness minimum if

$$\left.\frac{\partial^2 w(y,x^*)}{\partial y^2}\right|_{y=x^*} > 0 \tag{B3}$$

and a local maximum if the inequality is reversed. If the singular point is a local maximum of the fitness landscape, the corresponding singular trait value cannot be invaded by any nearby mutant. If such a trait value is also an attractor of the evolutionary dynamics, it is a final stop of evolution. If, however, the singular trait value is a minimum of the fitness landscape, it can be invaded by nearby mutants. Singular points that are both an attractor of the evolutionary dynamics and invadable are known as evolutionary branching points (Metz et al. 1996; Geritz et al. 1998). In conclusion, in the neighborhood of an evolutionary branching point, monomorphic populations experience directional selection towards this point and once the evolutionary dynamics is sufficiently close selection turns disruptive. Then, invading mutants are able to coexist with the resident at the evolutionary branching point – a dimorphism has evolved. Selection on this dimorphism continues to be divergent and thus leads to increased genetic variance (see figure C1 for more information). Importantly, such a stable pair of residents cannot be replaced by any mutant with intermediate phenotype.

In our model, invasion fitness (equation 6) can also be written as

$$w(y,x) = \lim_{T\to\infty} \frac{1}{T} \ln \left(\underline{\mathrm{u}} \prod_{t=1}^{T} \mathsf{L}(y, x, \theta_{1t}, .., \theta_{nt}) \underline{\mathrm{v}} \right) \tag{B4}$$

(Tuljapurkar 1990), where $\mathsf{L}(y, x, \theta_{1t}, .., \theta_{nt})$ is defined in equation (4). If we exclude the trivial case $m = 0$, invasion fitness as given by equation (B4) is independent of the entries in the row vector $\underline{\mathrm{u}}$ and the column vector $\underline{\mathrm{v}}$ as long as they are non-negative. Hence, below we can make convenient choices for these vectors. Note that in equation (B4) population projection matrices are multiplied from the left with increasing t.

Table B1: Shorthand notations used in the appendices.

population projection matrix	$\mathsf{L}(y, x, \theta_{1t}, .., \theta_{nt})$	$\rightarrow$	L_t
relative reproductive success	$\rho(y, x, \theta_{it})$	$\rightarrow$	ρ_{it}
first derivative	$\frac{\partial}{\partial y} a$	$\rightarrow$	∂a
second derivatives	$\frac{\partial^2}{\partial y^2} a$	$\rightarrow$	$\partial^2 a$
	$\frac{\partial^2}{\partial x \partial y} a$	$\rightarrow$	$\partial_x \partial_y a$
evaluation at singular trait value	$a\vert_{y=x=x^*}$	$\rightarrow$	a^*

Note: Here, a can be any function of the mutant and resident trait value. See table 1 for general notation.

B.1. Singular points

To keep the following derivations concise, we introduce the shorthand notations given in table B1. From the condition for a singular point (B1) we obtain with equation (B4)

$$0 = \frac{\partial w(y,x^*)}{\partial y}\bigg|_{y=x^*} = \lim_{T\to\infty}\frac{1}{T}\left(\frac{1}{\xi_T}\sum_{\tau=1}^{T}\underline{\mathrm{u}}\prod_{t_2=\tau+1}^{T}\mathsf{L}_{t_2}\partial\mathsf{L}_\tau\prod_{t_1=1}^{\tau-1}\mathsf{L}_{t_1}\underline{\mathrm{v}}\right)^*, \tag{B5}$$

where

$$\xi_T = \underline{\mathrm{u}}\prod_{t=1}^{T}\mathsf{L}_t\underline{\mathrm{v}}. \tag{B6}$$

Evaluating at $y = x = x^*$, the matrix L_t^* has the entries

$$l_{ij}^* = (1-\gamma)mc_j \text{ for } j \neq i \tag{B7a}$$

$$l_{ii}^* = 1-(1-\gamma)m\,(1-c_i)\,. \tag{B7b}$$

Hence, L_t^* is independent of x^* and t and equation (B5) simplifies to

$$0 = \lim_{T\to\infty}\frac{1}{T}\frac{1}{\xi_T^*}\sum_{\tau=1}^{T}\underline{\mathrm{u}}(\mathsf{L}^*)^{T-\tau}(\partial\mathsf{L}_\tau)^*(\mathsf{L}^*)^{\tau-1}\underline{\mathrm{v}}. \tag{B8}$$

Note that L^* is a stochastic matrix, i.e., the entries in each row sum up to one. We choose $\underline{\mathrm{u}}$ and $\underline{\mathrm{v}}$ to be the leading left and right eigenvectors of L^* to the eigenvalue one. The elements of these eigenvectors are $u_i = c_i$ and $v_i = 1$, respectively, and we obtain $\xi_T^* = \underline{\mathrm{u}}\mathsf{L}^*\underline{\mathrm{v}} = 1$. Equation (B8) simplifies to

$$0 = \lim_{T\to\infty}\frac{1}{T}\sum_{\tau=1}^{T}\underline{\mathrm{u}}(\partial\mathsf{L}_\tau)^*\underline{\mathrm{v}} \tag{B9}$$

Note that we can write

$$\underline{\mathrm{u}}(\partial\mathsf{L}_\tau)^*\underline{\mathrm{v}} = \sum_{i=1}^{n}\sum_{j=1}^{n}u_i(\partial l_{ij_\tau})^*v_j = (1-\gamma)\sum_{i=1}^{n}c_i(\partial\rho_{i\tau})^*. \tag{B10}$$

With the definitions of spatial and temporal expectation given in equation (7) and (8), equation (B5) becomes

$$\mathrm{E_T}\left[\mathrm{E_S}\left[(\partial\rho)^*\right]\right] = 0. \tag{B11}$$

Expressing this equation in terms of the local selection gradient $s_{it} = \ln\rho_{it}$ gives equation (11).

B.2. Invadability

A singular point x^* is invadable if inequality (B3) is fulfilled. Analogously to above we obtain

$$\left.\frac{\partial^2 w(y,x^*)}{\partial y^2}\right|_{y=x^*} = \lim_{T\to\infty}\frac{1}{T}\left(\partial\left(\underbrace{\frac{1}{\xi_T}\sum_{\tau=1}^{T}\underline{\mathsf{u}}\prod_{t_2=\tau+1}^{T}\mathsf{L}_{t_2}\partial\mathsf{L}_\tau\prod_{t_1=1}^{\tau-1}\mathsf{L}_{t_1}\underline{\mathsf{v}}}_{=:\zeta_{y,T}}\right)\right)^*, \tag{B12}$$

where ξ_T is given by equation (B6). This derivative can be rewritten as

$$\begin{aligned}\left.\frac{\partial^2 w(y,x^*)}{\partial y^2}\right|_{y=x^*} = \lim_{T\to\infty}\frac{1}{T}\Bigg(&-\frac{\zeta_{y,T}^2}{\xi_T^2}+\frac{1}{\xi_T}\sum_{\tau=1}^{T}\underline{\mathsf{u}}\prod_{t_2=\tau+1}^{T}\mathsf{L}_{t_2}\partial^2\mathsf{L}_\tau\prod_{t_1=1}^{\tau-1}\mathsf{L}_{t_1}\underline{\mathsf{v}}\\&+\frac{1}{\xi_T}\sum_{\tau_1=1}^{T}\sum_{\tau_2=\tau_1+1}^{T}\underline{\mathsf{u}}\prod_{t_3=\tau_2+1}^{T}\mathsf{L}_{t_3}\partial\mathsf{L}_{\tau_2}\prod_{t_2=\tau_1+1}^{\tau_2-1}\mathsf{L}_{t_2}\partial\mathsf{L}_{\tau_1}\prod_{t_1=1}^{\tau_1-1}\mathsf{L}_{t_1}\underline{\mathsf{v}}\\&+\frac{1}{\xi_T}\sum_{\tau_1=1}^{T}\sum_{\tau_2=1}^{\tau_1-1}\underline{\mathsf{u}}\prod_{t_3=\tau_1+1}^{T}\mathsf{L}_{t_3}\partial\mathsf{L}_{\tau_1}\prod_{t_2=\tau_2+1}^{\tau_1-1}\mathsf{L}_{t_2}\partial\mathsf{L}_{\tau_2}\prod_{t_1=1}^{\tau_2-1}\mathsf{L}_{t_1}\underline{\mathsf{v}}\Bigg)^*.\end{aligned} \tag{B13}$$

Analogously to the derivation of the singular point, we choose $\underline{\mathsf{u}}$ and $\underline{\mathsf{v}}$ to have elements $u_i = c_i$ and $v_i = 1$. Then $\xi^* = \underline{\mathsf{u}}\mathsf{L}^*\underline{\mathsf{v}} = 1$, and noting that the last two terms in equation (B13) are equal to each other, we get for the right-hand side

$$\lim_{T\to\infty}\frac{1}{T}\left[-\left(\sum_{\tau=1}^{T}\underline{\mathsf{u}}(\partial\mathsf{L}_\tau)^*\underline{\mathsf{v}}\right)^2+\sum_{\tau=1}^{T}\underline{\mathsf{u}}(\partial^2\mathsf{L}_\tau)^*\underline{\mathsf{v}}+2\sum_{\tau_1=1}^{T}\sum_{\tau_2=1}^{\tau_1-1}\underline{\mathsf{u}}(\partial\mathsf{L}_{\tau_1})^*\mathsf{L}^{*\tau_1-1-\tau_2}(\partial\mathsf{L}_{\tau_2})^*\underline{\mathsf{v}}\right]. \tag{B14}$$

We use equation (B10) and the analogue for the second derivative with respect to y to obtain

$$\begin{aligned}\left.\frac{\partial^2 w(y,x^*)}{\partial y^2}\right|_{y=x^*} = \lim_{T\to\infty}\frac{1}{T}\Bigg[&-\left(\sum_{\tau=1}^{T}(1-\gamma)\sum_{i=1}^{n}c_i(\partial\rho_{i\tau})^*\right)^2+\sum_{\tau=1}^{T}(1-\gamma)\sum_{i=1}^{n}c_i(\partial^2\rho_{i\tau})^*\\&+2\sum_{\tau_1=1}^{T}\sum_{\tau_2=1}^{\tau_1-1}\underline{\mathsf{u}}(\partial\mathsf{L}_{\tau_2})^*\mathsf{L}^{*\tau_1-1-\tau_2}(\partial\mathsf{L}_{\tau_1})^*\underline{\mathsf{v}}\Bigg].\end{aligned} \tag{B15}$$

Calculating the squared term and identifying temporal and spatial averages as defined in equation (7) and (8), we get

$$\begin{aligned}\left.\frac{\partial^2 w(y,x^*)}{\partial y^2}\right|_{y=x^*} =&-(1-\gamma)^2\left(\mathrm{E_T}\left[\mathrm{E_S}\left[(\partial\rho)^*\right]^2\right]+\lim_{T\to\infty}\frac{1}{T}\sum_{\tau_1=1}^{T}\sum_{\substack{\tau_2=1\\\tau_2\neq\tau_1}}^{T}\mathrm{E_S}\left[(\partial\rho_{\tau_1})^*\right]\mathrm{E_S}\left[(\partial\rho_{\tau_2})^*\right]\right)\\&+(1-\gamma)\mathrm{E_T}\left[\mathrm{E_S}\left[(\partial^2\rho)^*\right]\right]+2\lim_{T\to\infty}\frac{1}{T}\sum_{\tau_1=1}^{T}\sum_{\tau_2=1}^{\tau_1-1}\underline{\mathsf{u}}(\partial\mathsf{L}_{\tau_2})^*\mathsf{L}^{*\tau_1-1-\tau_2}(\partial\mathsf{L}_{\tau_1})^*\underline{\mathsf{v}}.\end{aligned} \tag{B16}$$

Noting that we can write

$$\mathsf{L}^* = \mathbb{I} + m(1-\gamma)(\underline{\mathrm{v}}\underline{\mathrm{u}} - \mathbb{I}), \tag{B17}$$

where $\mathbb{I}$ is the identity matrix and $\underline{\mathrm{v}}\underline{\mathrm{u}}$ is the tensor product, i.e., a matrix with elements $[\underline{\mathrm{v}}\underline{\mathrm{u}}]_{ij} = v_i u_j = c_j$, we can calculate

$$\mathsf{L}^{*\tau} = (1 - m(1-\gamma))^\tau (\mathbb{I} - \underline{\mathrm{v}}\underline{\mathrm{u}}) + \underline{\mathrm{v}}\underline{\mathrm{u}}. \tag{B18}$$

Here, we have used the binomial theorem and that $(\underline{\mathrm{v}}\underline{\mathrm{u}})^k = \underline{\mathrm{v}}\underline{\mathrm{u}}$ for $k > 0$. Furthermore,

$$\underline{\mathrm{u}}(\partial \mathsf{L}_{\tau_2})^* = \underline{\mathrm{u}}\left(\mathsf{L}^* - \gamma\mathbb{I}\right)\mathbb{I}\left[(\partial\rho_{\tau_2})^*\right] = (1-\gamma)\underline{\mathrm{u}}\mathbb{I}\left[(\partial\rho_{\tau_2})^*\right] \tag{B19a}$$

$$(\partial \mathsf{L}_{\tau_1})^*\underline{\mathrm{v}} = \left(\mathsf{L}^* - \gamma\mathbb{I}\right)\mathbb{I}\left[(\partial\rho_{\tau_1})^*\right]\underline{\mathrm{v}}, \tag{B19b}$$

where $\mathbb{I}\left[a\right]$ is a diagonal matrix with a_i at position i. Using equations (B18) and (B19), the last term in equation (B16) calculates to

$$\begin{aligned}
&2\lim_{T\to\infty}\frac{1}{T}\sum_{\tau_1=1}^{T}\sum_{\tau_2=1}^{\tau_1-1}(1-\gamma)\underline{\mathrm{u}}\mathbb{I}\left[(\partial\rho_{\tau_2})^*\right]\mathsf{L}^{*\tau_1-1-\tau_2}\left(\mathsf{L}^* - \gamma\mathbb{I}\right)\mathbb{I}\left[(\partial\rho_{\tau_1})^*\right]\underline{\mathrm{v}} = \\
&2(1-\gamma)^2\left(\lim_{T\to\infty}\frac{1}{T}\sum_{\tau_1=1}^{T}\sum_{\tau_2=1}^{\tau_1-1}\left(\underline{\mathrm{u}}\mathbb{I}\left[(\partial\rho_{\tau_1})^*\right]\underline{\mathrm{v}}\right)\left(\underline{\mathrm{u}}\mathbb{I}\left[(\partial\rho_{\tau_2})^*\right]\underline{\mathrm{v}}\right) + \right. \\
&\left.(1-m)\lim_{T\to\infty}\frac{1}{T}\sum_{\tau_1=1}^{T}\sum_{\tau_2=1}^{\tau_1-1}(1-m(1-\gamma))^{\tau_1-1-\tau_2}\left(\underline{\mathrm{u}}\mathbb{I}\left[(\partial\rho_{\tau_1})^*(\partial\rho_{\tau_2})^*\right]\underline{\mathrm{v}} - \left(\underline{\mathrm{u}}\mathbb{I}\left[(\partial\rho_{\tau_2})^*\right]\underline{\mathrm{v}}\right)\left(\underline{\mathrm{u}}\mathbb{I}\left[(\partial\rho_{\tau_1})^*\right]\underline{\mathrm{v}}\right)\right)\right).
\end{aligned} \tag{B20}$$

Using that $\underline{\mathrm{u}}\mathbb{I}[a]\underline{\mathrm{v}} = \mathrm{E_S}[a]$, the first term in this expression becomes

$$2(1-\gamma)^2\sum_{\tau_1=1}^{T}\sum_{\tau_2=1}^{\tau_1-1}\mathrm{E_S}\left[(\partial\rho_{\tau_1})^*\right]\mathrm{E_S}\left[([\partial\rho_{\tau_2})^*\right] = (1-\gamma)^2\sum_{\tau_1=1}^{T}\sum_{\substack{\tau_2=1\\ \tau_2\neq\tau_1}}^{T}\mathrm{E_S}\left[(\partial\rho_{\tau_1})^*\right]\mathrm{E_S}\left[(\partial\rho_{\tau_2})^*\right], \tag{B21}$$

where we have used that the $(\partial\rho_{i\tau})^*$ have a stationary distribution. This term precisely cancels with the second term in equation (B16). The last term in expression (B20) can be identified as a spatial covariance,

$$2(1-\gamma)^2(1-m)\lim_{T\to\infty}\frac{1}{T}\sum_{\tau_1=1}^{T}\sum_{\tau_2=1}^{\tau_1-1}(1-m(1-\gamma))^{\tau_1-1-\tau_2}\mathrm{Cov_S}[(\partial\rho_{\tau_2})^*, (\partial\rho_{\tau_1})^*]. \tag{B22}$$

This term contains the spatial covariance between $(\partial\rho_i)^*$ at two points in time, summed over all possible pairs of time points. Under our time-invariance assumption of the environmental process, covariance terms depend only on time differences $\tau = \tau_1 - \tau_2$. The outer sum can then be written as a weighting factor to the terms of the inner sum and we obtain

$$2(1-\gamma)^2(1-m)\lim_{T\to\infty}\sum_{\tau=1}^{T-1}(1-\frac{\tau}{T})(1-m(1-\gamma))^{\tau-1}\mathrm{E_T}[\mathrm{Cov_S}[(\partial\rho_t)^*, (\partial\rho_{t+\tau})^*]], \tag{B23}$$

In the limit $T \to \infty$ this becomes

$$2(1-\gamma)^2(1-m)\sum_{\tau=1}^{\infty}(1-m(1-\gamma))^{\tau-1}\mathrm{E_T}[\mathrm{Cov_S}[(\partial\rho_t)^*,(\partial\rho_{t+\tau})^*]] = 2(1-\gamma)\frac{1-m}{m}\mathrm{Var_S}\left[\mathrm{E_T}\left[(\partial\rho)^*\right]\right] +$$
$$2(1-\gamma)^2(1-m)\sum_{\tau=1}^{\infty}(1-m(1-\gamma))^{\tau-1}\left(\mathrm{E_S}\left[\mathrm{Cov_T}\left[(\partial\rho_t)^*,(\partial\rho_{t+\tau})^*\right]\right] - \mathrm{Cov_T}\left[\mathrm{E_S}\left[(\partial\rho_t)^*\right],\mathrm{E_S}\left[(\partial\rho_{t+\tau})^*\right]\right]\right), \tag{B24}$$

where the index t is kept for clarity where necessary. For the right-hand side of equation (B24) we used the definition of the covariance, $\mathrm{Cov}[a,b] = \mathrm{E}[ab] - \mathrm{E}[a]\mathrm{E}[b]$, and the relations $\mathrm{E_T}[\mathrm{E_S}[a]] = \mathrm{E_S}[\mathrm{E_T}[a]]$ and $\mathrm{E_T}[(\partial\rho_{it})^*] = \mathrm{E_T}[(\partial\rho_{it+\tau})^*]$. The transformation applied here reflects the fact that spatial covariance between the $(\partial\rho_{i.})^*$ at different points in time can be produced by two factors. First, differences in the probability distribution of environmental conditions between patches produce spatial covariance. This contribution is independent of τ. Second, spatial covariance is produced by temporal correlations in environmental conditions.

Going back to the the second derivative of invasion fitness, equation (B16), we can reformulate the first and third term using

$$\mathrm{E_T}\left[\mathrm{E_S}\left[(\partial\rho)^*\right]^2\right] = \mathrm{E_T}\left[\mathrm{E_S}\left[(\partial\rho)^*\right]\right]^2 + \mathrm{Var_T}\left[\mathrm{E_S}\left[(\partial\rho)^*\right]\right], \tag{B25}$$

and

$$\mathrm{E_S}\left[(\partial\rho)^*\right]^2 = \mathrm{E_S}\left[(\partial\rho)^{*2}\right] - \mathrm{Var_S}\left[(\partial\rho)^*\right], \tag{B26}$$

where it follows from equation (11) that the first term on the right-hand side of equation (B25) is zero. With equations (B21)-(B26), we can write equation (B16) as

$$\left.\frac{\partial^2 w(y,x^*)}{\partial y^2}\right|_{y=x^*} = (1-\gamma)\left(\mathrm{E_T}\left[\mathrm{E_S}\left[(\partial^2\rho)^* - (\partial\rho)^{*2}\right]\right] + \mathrm{E_T}\left[\mathrm{Var_S}\left[(\partial\rho)^*\right]\right] + \gamma\mathrm{Var_T}\left[\mathrm{E_S}\left[(\partial\rho)^*\right]\right]\right.$$
$$\left. +2(1-\gamma)(1-m)\sum_{\tau=1}^{\infty}(1-m(1-\gamma))^{\tau-1}\mathrm{E_T}\left[\mathrm{Cov_S}\left[(\partial\rho_t)^*,(\partial\rho_{t+\tau})^*\right]\right]\right) =$$
$$(1-\gamma)\left(\mathrm{E_T}\left[\mathrm{E_S}\left[(\partial^2\rho)^* - ((\partial\rho)^*)^2\right]\right] + \mathrm{E_T}\left[\mathrm{Var_S}\left[(\partial\rho)^*\right]\right] + \gamma\mathrm{Var_T}\left[\mathrm{E_S}\left[(\partial\rho)^*\right]\right] + 2\frac{1-m}{m}\mathrm{Var_S}\left[\mathrm{E_T}\left[(\partial\rho)^*\right]\right] +\right.$$
$$\left. 2(1-\gamma)(1-m)\sum_{\tau=1}^{\infty}(1-m(1-\gamma))^{\tau-1}\left(\mathrm{E_S}\left[\mathrm{Cov_T}\left[(\partial\rho_t)^*,(\partial\rho_{t+\tau})^*\right]\right] - \mathrm{Cov_T}\left[\mathrm{E_S}\left[(\partial\rho_t)^*\right],\mathrm{E_S}\left[(\partial\rho_{t+\tau})^*\right]\right]\right)\right), \tag{B27}$$

where the second version is longer, but easier to interpret (see results section and discussion). With $s_{it} := \ln(\rho_{it})$ and noting that $(\partial s_{it})^* = (\partial\rho_{it})^*$ and $(\partial^2 s_{it})^* = (\partial^2\rho_{it})^* - ((\partial\rho_{it})^*)^2$, we can write condition (B3) as given in equation (14).

B.3. Gaussian selection

For Gaussian stabilizing selection towards a selective optimum θ_{it}, the functions $r(x,\theta_{it})$ in $\rho_{it} = \exp(s_{it}) = \frac{r(y,\theta_{it})}{r(x,\theta_{it})}$ are given by equation (1) and we obtain

$$(\partial_y \rho_{it})^* = (\partial_y s_{it})^* = \frac{\theta_{it} - x^*}{\sigma^2}, \tag{B28}$$

$$(\partial_y^2 \rho_{it})^* = \frac{(\theta_{it} - x^*)^2}{\sigma^4} - \frac{1}{\sigma^2}, \tag{B29}$$

$$(\partial_y^2 s_{it})^* = -\frac{1}{\sigma^2}. \tag{B30}$$

With this, conditions (12) and (15) easily follow from conditions (11) and (14), respectively.

B.4. Convergence stability

In this section, we use subscripts y and x to distinguish derivatives with respect to mutant and resident, respectively. A singular point is an attractor of the evolutioary dynamics if inequality (B2) is fulfilled. This inequality can be written as

$$\left.\frac{\partial^2 w(y,x)}{\partial x \partial y}\right|_{y=x=x^*} + \left.\frac{\partial^2 w(y,x^*)}{\partial y^2}\right|_{y=x^*} < 0 \tag{B31}$$

(Geritz et al. 1998), where the double derivative with respect to y is given by equation (B27). The mixed derivative equals

$$\begin{aligned}
\left.\frac{\partial^2 w(y,x)}{\partial x \partial y}\right|_{y=x=x^*} &= \lim_{T\to\infty} \frac{1}{T} \left(\partial_x \left(\underbrace{\frac{1}{\xi_T} \sum_{\tau=1}^{T} \underline{\mathsf{u}} \prod_{t_1=\tau+1}^{T} \mathsf{L}_{\mathsf{t}_1} \partial_y \mathsf{L}_\tau \prod_{t_2=1}^{\tau-1} \mathsf{L}_{\mathsf{t}_2} \underline{\mathsf{v}}}_{=:\zeta_{y,T}} \right) \right)^* \\
&= \lim_{T\to\infty} \frac{1}{T} \left(-\frac{\zeta_{y,T}\zeta_{x,T}}{\xi_T^2} + \frac{1}{\xi_T} \sum_{\tau=1}^{T} \underline{\mathsf{u}} \prod_{t_1=\tau+1}^{T} \mathsf{L}_{t_1} \partial_x \partial_y \mathsf{L}_\tau \prod_{t_2=1}^{\tau-1} \mathsf{L}_{t_1} \underline{\mathsf{v}} \right. \\
&\quad + \frac{1}{\xi_T} \sum_{\tau_1=1}^{T} \sum_{\tau_2=\tau_1+1}^{T} \underline{\mathsf{u}} \prod_{t_1=\tau_2+1}^{T} \mathsf{L}_{t_1} \partial_x \mathsf{L}_{\tau_2} \prod_{t_2=\tau_1+1}^{\tau_2-1} \mathsf{L}_{t_2} \partial_y \mathsf{L}_{\tau_1} \prod_{t_3=1}^{\tau_1-1} \mathsf{L}_{t_3} \underline{\mathsf{v}} \\
&\quad \left. + \frac{1}{\xi_T} \sum_{\tau_1=1}^{T} \sum_{\tau_2=1}^{\tau_1-1} \underline{\mathsf{u}} \prod_{t_1=\tau_1+1}^{T} \mathsf{L}_{t_1} \partial_y \mathsf{L}_{\tau_1} \prod_{t_2=\tau_2+1}^{\tau_1-1} \mathsf{L}_{t_2} \partial_x \mathsf{L}_{\tau_2} \prod_{t_3=1}^{\tau_2-1} \mathsf{L}_{t_3} \underline{\mathsf{v}} \right)^*.
\end{aligned} \tag{B32}$$

Here, $\zeta_{x,T}$ is the same as $\zeta_{y,T}$ except that the derivative of L_t is with respect to the resident trait value x. Using analogous simplifications as in the calculations above, we obtain

$$\begin{aligned}\frac{\partial^2 w(y,x)}{\partial x \partial y}\Big|_{y=x=x^*} = \lim_{T\to\infty}\frac{1}{T}\Bigg[&-\left(\sum_{\tau=1}^{T}(1-\gamma)\sum_{i=1}^{n}(\partial_y\rho_{i\tau})^*\right)\left(\sum_{\tau=1}^{T}(1-\gamma)\sum_{i=1}^{n}(\partial_x\rho_{i\tau})^*\right)+\\ &\sum_{\tau=1}^{T}(1-\gamma)\sum_{i=1}^{n}(\partial_x\partial_y\rho_{i\tau})^*+\sum_{\tau_1=1}^{T}\sum_{\tau_2=\tau_1+1}^{T}\underline{\mathrm{u}}(\partial_x\mathsf{L}_{\tau_1})^*\mathsf{L}^{*\tau_2-1-\tau_1}(\partial_y\mathsf{L}_{\tau_2})^*\underline{\mathrm{v}}+\\ &\sum_{\tau_1=1}^{T}\sum_{\tau_2=1}^{\tau_1-1}\underline{\mathrm{u}}(\partial_y\mathsf{L}_{\tau_1})^*\mathsf{L}^{*\tau_2-1-\tau_1}(\partial_x\mathsf{L}_{\tau_2})^*\underline{\mathrm{v}}\Bigg].\end{aligned} \tag{B33}$$

Using that

$$(\partial_x\mathsf{L}_\tau)^* = -(\partial_y\mathsf{L}_\tau)^*,\ (\partial_x\rho_{i\tau})^* = -(\partial_y\rho_{i\tau})^* \text{ and } (\partial_x\partial_y\rho_{i\tau})^* = -(\partial_y^2\rho_{i\tau})^*, \tag{B34}$$

we obtain

$$\begin{aligned}\frac{\partial^2 w(y,x)}{\partial y \partial x}\Big|_{y=x=x^*} = \lim_{T\to\infty}\frac{1}{T}\Bigg[&\left(\sum_{\tau=1}^{T}\left((1-\gamma)\sum_{i=1}^{n}(\partial_y\rho_{i\tau})^*\right)\right)^2-\sum_{\tau=1}^{T}(1-\gamma)\sum_{i=1}^{n}{(\partial_y^2\rho_{i\tau})^*}^2\\ &-2\sum_{\tau_1=1}^{T}\sum_{\tau_2=\tau_1+1}^{T}\underline{\mathrm{u}}(\partial_y\mathsf{L}_{\tau_1})^*\mathsf{L}^{*\tau_2-1-\tau_1}(\partial_y\mathsf{L}_{\tau_2})^*\underline{\mathrm{v}}\Bigg].\end{aligned} \tag{B35}$$

Combining equations (B15) and (B35), condition (B31) becomes

$$(1-\gamma)\lim_{T\to\infty}\frac{1}{T}\left[\sum_{\tau=1}^{T}\sum_{i=1}^{n}(\partial_y^2\rho_{i\tau})^*-{(\partial_y\rho_{i\tau})^*}^2\right] = \mathrm{E_T}\left[\mathrm{E_S}\left[(\partial_y^2\rho)^*\right]-\mathrm{E_S}\left[{(\partial_y\rho)^*}^2\right]\right]<0. \tag{B36}$$

Expressing this inequality in terms of s results in equation (13).

C. Appendix: Special cases and extensions

C.1. Uncorrelated patches

Here, we derive equation (17) from the main text. If we assume that there are no correlations in environmental conditions across patches, the probability density function can be written as

$$f(\theta_1,..,\theta_n) = \prod_{i=1}^{n} f_i(\theta_i),$$

where $f_i(\theta_i)$ is the probability distribution of environmental condition θ_i in patch i. In the following, we write $f_i := f_i(\theta_i)$. Then the first term on the left-hand side of condition (14) can be written as

$$\mathrm{E_T}\left[\mathrm{Var_S}\left[(\partial_y s)^*\right]\right] = \int_{-\infty}^{\infty}...\int_{-\infty}^{\infty}\left(\prod_{i=1}^{n} f_i\right)\left[\sum_{i=1}^{n} c_i{(\partial_y s_i)^*}^2-\sum_{i=1}^{n}\sum_{j=1}^{n}c_i c_j(\partial_y s_i)^*(\partial_y s_j)^*\right]\mathrm{d}\theta_1...\mathrm{d}\theta_n. \tag{C1}$$

Since the environmental conditions in the patches are independent, the ith term in the first sum is a constant with respect to all integration variables except θ_i, and the (i,j)th term in the second sum is a constant with respect to all integration variables except θ_i and θ_j. Noting that $\int f_k \mathrm{d}\theta_k = 1$, we can simplify by exchanging the distribution averaging and the averaging over the patches. For the last term in equation (C1) we have to distinguish between the indices $i = j$, where the optimum is the same, and $i \neq j$, for which patches are independent. With this we get

$$\begin{aligned}\mathrm{E_T}\left[\mathrm{Var_S}\left[(\partial_y s)^*\right]\right] = &\sum_{i=1}^{n} c_i \int_{-\infty}^{\infty} f_i (\partial_y s_i)^{*2} \mathrm{d}\theta_i - \sum_{i=1}^{n} c_i^2 \int_{-\infty}^{\infty} f_i (\partial_y s_i)^{*2} \mathrm{d}\theta_i \\ &- \sum_{i=1}^{n} c_i \sum_{\substack{j=1 \\ j\neq i}}^{n} c_j \int_{-\infty}^{\infty}\int_{-\infty}^{\infty} f_i f_j (\partial_y s_i)^* (\partial_y s_j)^* \mathrm{d}\theta_i \mathrm{d}\theta_j .\end{aligned} \tag{C2}$$

Here, the first term comes from the first term in brackets on the right-hand side of equation (C1), the middle term is the part of the last term from equation (C1) where $i = j$ and the last term is the one where $i \neq j$. With the definition of the temporal average (equation 9), this becomes

$$\mathrm{E_T}\left[\mathrm{Var_S}\left[(\partial_y s)^*\right]\right] = \sum_{i=1}^{n} c_i \mathrm{E_T}\left[(\partial_y s_i)^{*2}\right] - \sum_{i=1}^{n} c_i^2 \mathrm{E_T}\left[(\partial_y s_i)^{*2}\right] - \sum_{i=1}^{n} c_i \mathrm{E_T}\left[(\partial_y s_i)^*\right] \sum_{\substack{j=1 \\ j\neq i}}^{n} c_j \mathrm{E_T}\left[(\partial_y s_j)^*\right]. \tag{C3}$$

Using that $\mathrm{E_T}[b^2] = \mathrm{Var_T}[b] + \mathrm{E_T}[b]^2$ for any b and with the definition of the spatial average (equation 7), we obtain after rearranging

$$\mathrm{E_T}\left[\mathrm{Var_S}\left[(\partial_y s)^*\right]\right] = \mathrm{E_S}\left[(1-c)\,\mathrm{Var_T}\left[(\partial_y s)^*\right]\right] + \mathrm{Var_S}\left[\mathrm{E_T}\left[(\partial_y s)^*\right]\right], \tag{C4}$$

where we omit the patch index of c_i inside the spatial average. We can apply steps analogous to (C1)-(C4) to reformulate the second term on the left-hand side of inequality (14) and get

$$\mathrm{Var_T}\left[\mathrm{E_S}\left[(\partial_y s)^*\right]\right] = \sum_{i=1}^{n} c_i^2 \mathrm{E_T}[(\partial_y s_i)^{*2}] + \sum_{i=1}^{n} c_i \mathrm{E_T}[(\partial_y s_i)^*] \sum_{\substack{j=1 \\ j\neq i}}^{n} c_j \mathrm{E_T}[(\partial_y s_j)^*] - \mathrm{E_S}[\mathrm{E_T}[(\partial_y s)^*]]^2, \tag{C5}$$

where the middle term on the right-hand side is the same as the last term in (C3) and can be rearranged as above. With the definition of the spatial average we get

$$\mathrm{Var_T}[\mathrm{E_S}[(\partial_y s)^*]] = \mathrm{E_S}\left[c\mathrm{Var_T}[(\partial_y s)^*]\right]. \tag{C6}$$

In the absence of temporal correlations, the term $\mathcal{C}\left[(\partial_y s)^*\right]$ in condition (14) equals zero. Hence, for uncorrelated patches the condition for invadability, inequality (14), can be rewritten as

$$\begin{aligned}&\mathrm{Var_S}\left[\mathrm{E_T}\left[(\partial_y s)^*\right]\right] + \mathrm{E_S}\left[(1-c)\,\mathrm{Var_T}\left[(\partial_y s)^*\right]\right] \\ &+\gamma \mathrm{E_S}\left[c\mathrm{Var_T}\left[(\partial_y s)^*\right]\right] + 2\frac{1-m}{m}\mathrm{Var_S}\left[\mathrm{E_T}\left[(\partial_y s)^*\right]\right] > -\mathrm{E_T}\left[\mathrm{E_S}\left[(\partial_y^2 s)^*\right]\right].\end{aligned} \tag{C7}$$

This can be further simplified by using the definition of the covariance, $\mathrm{Cov}[a,b] = \mathrm{E}[ab] - \mathrm{E}[a]\mathrm{E}[b]$, and that $\mathrm{E_S}[c] = 1/n$. We obtain

$$\frac{2-m}{m}\mathrm{Var_S}\left[\mathrm{E_T}\left[(\partial_y s)^*\right]\right] + \left(1 - \frac{1-\gamma}{n}\right)\mathrm{E_S}\left[\mathrm{Var}_T\left[(\partial_y s)^*\right]\right] - (1-\gamma)\mathrm{Cov_S}\left[c, \mathrm{Var_T}\left[(\partial_y s)^*\right]\right] > -\mathrm{E_T}\left[\mathrm{E_S}\left(\partial_y^2 s)^*\right]\right], \tag{C8}$$

which for the Gaussian case becomes condition (17). It can be informative to consider the origin of the the terms in condition (C8) with respect to the original branching condition, inequality (14). For the case of Gaussian selection and equally sized patches ($c_i = 1/n$), we have

$$\overbrace{\mathrm{Var_S}[\mathrm{E_T}[\theta]] + \left(1 - \frac{1}{n}\right)\mathrm{E_S}\left[\mathrm{Var_T}[\theta]\right]}^{\mathrm{E_T}[\mathrm{Var_S}[\theta]]=} + \overbrace{\frac{\gamma}{n}\mathrm{E_S}\left[\mathrm{Var_T}[\theta]\right]}^{\gamma\mathrm{Var_T}[\mathrm{E_S}[\theta]]=} + 2\frac{1-m}{m}\mathrm{Var_S}[\mathrm{E_T}[\theta]] > \sigma^2, \tag{C9}$$

where the correspondence to terms in condition (15) is given above the braces. We see that the expected spatial variation results from two sources. The first source are differences in the expected environments among patches and the second source are temporal fluctuations within patches. These fluctuations lead to differences among patch optima for a given season. The second factor becomes increasingly important as the number of patches increases. The third term on the left-hand side of condition (C9) shows that temporal fluctuations within the patches contribute less to "global" temporal fluctuations as the patch number, n, increases. The reason is that local fluctuations average out over space.

C.2. Different strength of selection in the patches

Here we consider the case of Gaussian selection and relax the assumption that the strength of selection is identical for all patches. We denote by $1/\sigma_i$ the strength of selection in patch i. Then, inserting equation (B28) into equation (11) gives

$$0 = -x^* \sum_{i=1}^{n} c_i \frac{1}{\sigma_i^2} + \int_{\Omega} f(\theta_1, .., \theta_n) \sum_{i=1}^{n} c_i \frac{\theta_i}{\sigma_i^2} \mathrm{d}\theta_1 .. \mathrm{d}\theta_n, \tag{C10}$$

which, using the definition of the spatial average and solving for x^*, gives

$$x^* = \frac{\mathrm{E_T}\left[\mathrm{E_S}\left[\frac{\theta}{\sigma^2}\right]\right]}{\mathrm{E_S}\left[\frac{1}{\sigma^2}\right]}. \tag{C11}$$

For the branching condition we start with equation (14) and use the results from appendices B.2 and B.3, except that now the σ_i cannot be factored out from the spatial averages. In the absence

of temporal correlations, we get

$$\sum_{i=1}^{n} c_i \frac{1}{\sigma_i^2} < \int_{\Omega} f(\theta_1,..,\theta_n) \left[\sum_{i=1}^{n} c_i \left(\frac{\theta_i - x^*}{\sigma_i^2} \right)^2 - \left(\sum_{i=1}^{n} c_i \frac{\theta_i - x^*}{\sigma_i^2} \right)^2 \right] \mathrm{d}\theta_1..\mathrm{d}\theta_n$$
$$+ \gamma \int_{\Omega} f(\theta_1,..,\theta_n) \left(\sum_{i=1}^{n} c_i \frac{\theta_i - x^*}{\sigma_i^2} \right)^2 \mathrm{d}\theta_1..\mathrm{d}\theta_n + \sum_{i=1}^{n} c_i \left(\int_{\Omega} \frac{\theta_i - x^*}{\sigma_i^2} \mathrm{d}\theta_1..\mathrm{d}\theta_n \right)^2 - \left(\sum_{i=1}^{n} c_i \int_{\Omega} \frac{\theta_i - x^*}{\sigma_i^2} \mathrm{d}\theta_1..\mathrm{d}\theta_n \right)^2 . \tag{C12}$$

With the definition of the spatial variance and using equation (C11) we obtain the branching condition,

$$\mathrm{E_T}\left[\mathrm{Var_S}\left[\frac{\theta - x^*}{\sigma^2} \right] \right] + \gamma \mathrm{Var_T}\left[\mathrm{E_S}\left[\frac{\theta}{\sigma^2} \right] \right] + 2\frac{1-m}{m} \mathrm{Var_S}\left[\mathrm{E_T}\left[\frac{\theta}{\sigma^2} \right] \right] > \mathrm{E_S}\left[\frac{1}{\sigma^2} \right]. \tag{C13}$$

In this case, the terms in the calculation of the spatial mean and variance are weighted by $1/\sigma_i^2$. Thus, patches in which selection is strong contribute relatively more to the total variance in selective optima and thus to branching.

C.3. Special cases for Gaussian selection

From equation (15) (or equations C9 or 17 for independently distributed patches), σ^2_{crit} is readily computed for any combination of optima distributions. Empirically, the relevant expectations and variances can be estimated from sufficiently long time-series measurements. In the following we compute the branching condition for several relevant examples, starting from simple to more complex cases. For classical models we recover the known conditions.

C.3.1. No spatial differences

If the selective optimum is always equal across all patches, then the population effectively consists of a single patch. From equation (15) the branching condition becomes

$$\gamma \mathrm{Var_T}[\theta] > \sigma^2. \tag{C14}$$

For this special case we retrieve the lottery model of species coexistence (Chesson and Warner 1981), for which it is known that temporal fluctuations in selection can lead to the evolution and maintenance of genetic variance if there is generation overlap (Seger and Brockmann 1987). Our branching condition is consistent with earlier work (Ellner and Hairston 1994, equation 9; Svardal et al. 2011, equation 7).

C.3.2. No temporal fluctuations

If selective optima in the patches are fixed, then the time-averages in condition (12) and condition (17) disappear and the branching condition becomes

$$\frac{2-m}{m}\,\mathrm{Var_S}[\theta] = \frac{2-m}{m}\sum_{i=1}^{n}\sum_{\substack{j=1\\ j\neq i}}^{n} c_i c_j(\theta_i-\theta_j)^2 > \sigma^2. \tag{C15}$$

For the special case of the Levene model ($m = 1$), this equals Geritz et al.'s (1998) equation B8. The right-hand side of equation (C15) measures the sum of the squared pairwise differences between patches weighted by their relative output. Thus, for given difference between patches, the evolution and maintenance of genetic variation becomes more difficult if the patch sizes become more different. This is in accordance with results by Gillespie (1974).

C.3.3. Independently and identically distributed optima with two possible states

If the occurrence of environmental conditions follows an identical distribution in all patches, then the first term on the right-hand side of equation (C9) equals zero. Here, we focus on the case that all patches are of identical size and can take the selective optima θ_A and θ_B, with probabilities p and $1-p$, respectively. We assume that spatial correlations are absent. Using equation (C9), we find for the branching condition

$$\left(1-\frac{1-\gamma}{n}\right)(\theta_A-\theta_B)^2 p(1-p) > \sigma^2. \tag{C16}$$

In the limit of infinitely many patches we retrieve the condition for the Levene model (equation (C15) with $m = 1$ and 2 patches of relative sizes p and $1-p$). This is because the realized frequency of patch types in a given year approaches the expected frequency. For two patches and $\gamma = 0$, the right-hand side of equation (C16) is reduced by a factor 1/2 relative to the Levene model.

C.3.4. Known distributions of selective optima

If the distribution of the selective optima is known, then this information can be used to obtain an explicit expression for the left-hand side of equation (C9) or (17). For instance, if the selective optima in the patches are determined by many random processes of small effect, then they are approximately Gaussian distributed. Then $\mathrm{E_T}[\theta]$ and $\mathrm{Var_T}[\theta]$ are given by the mean and variance of the Gaussian distributions in each patch, $\mu_{\theta i}$ and $\sigma^2_{\theta i}$, respectively, and the branching condition for the case of equal juvenile carrying capacities is

$$\frac{1}{n}\sum_i \left(\mu_{\theta i}-\bar{\mu}_\theta\right)^2 + \frac{n-1+\gamma}{n^2}\sum_i \sigma^2_{\theta i} > \sigma^2, \tag{C17}$$

where $\bar{\mu}_\theta = \frac{1}{n}\sum \mu_{\theta i}$.

Another classic distribution is given when the optimum for the trait under consideration is determined by how often a certain event occurs during the selective period. This would for instance be the case if the optimum is determined by the number of predation events or the number of days with frost. If we assume that these events are independent and that they occur with a constant rate, then they are Poisson distributed. Also other environmental quantities such as the amount of rain per area are approximately Poisson distributed. In such cases, the branching condition is given by equation (C17) where $\mu_{\theta i}$ and $\sigma^2_{\theta i}$ are substituted by the rate parameter of the Poisson distribution.

C.3.5. Spatial correlations

It is straightforward to consider different patterns of spatial correlations in our framework. Here we give two simple examples for two equally sized patches with identically distributed environmental conditions. Furthermore, we assume that temporal autocorrelations are absent ($\mathcal{C}[\theta] = 0$ in condition 15). With this assumption, the third term on the left-hand side of condition (15) is independent of spatial correlations. Hence, we can assume without loss of generality that $m = 1$.

First, assume that the selective optima in the two patches are multivariate normal distributed with identical mean $\mu = 0$ and variance σ_e^2, and that there are correlations between the patches of strength ω_S. Then, the probability density function of the environmental state vector is given by

$$f(\theta_1, \theta_2) = \frac{1}{2\pi\sigma_e^2\sqrt{1-\omega_S^2}} \exp\left(-\frac{1}{2\sigma_e^2(1-\omega_S^2)}\left(\theta_1^2 + \theta_2^2 - 2\omega_S\theta_1\theta_2\right)\right). \tag{C18}$$

With this, the branching condition can be calculated from equation (15) as

$$\frac{\sigma_e^2}{2}(1 - \omega_S + \gamma(1+\omega_S)) > \sigma^2. \tag{C19}$$

We interpret this condition below.

Second, assume that the optima in the two patches are identically Bernoulli distributed. Specifically, we assume that in both patches the two selective optima θ_A and θ_B occur with probability $1/2$. We measure spatial correlation with a parameter $\omega_S \in [-1, 1]$. A value $\omega_S = 0$ indicates the absence of correlation. Positive values of ω_S linearly increase the probability that the two patches are equal in any generation and negative values linearly increase the probability that the patches are different. For $\omega_S = \pm 1$ the optima in the patches are always equal or different, respectively. The branching condition calculates to

$$\frac{1}{8}\left[(1-\omega_S) + \gamma(1+\omega_S)\right](\theta_A - \theta_B)^2 > \sigma^2. \tag{C20}$$

From both equation (C19) and (C20), we see that spatial correlations have opposite effects on two parts of σ^2_{crit}. First, positive (negative) correlations decrease (increase) spatial variance by making

the patches less (more) likely to be different. Second, positive (negative) correlations increase (decrease) the amount of global temporal fluctuations by making it more (less) likely that patches change in concert. The former effect always out-weights the latter so that positive (negative) correlations generally hinder (promote) the evolution of genetic diversity. However, the effect of correlations decreases with increasing generation overlap. Furthermore, for completely negatively correlated selective optima between the patches, we retrieve the case of the Levene model with two equally sized patches, for no correlation we obtain the case of two patches with identically and independently distributed selective optima from above, and for completely positively correlated patches we obtain the condition from the lottery model.

C.3.6. Temporal correlation

Temporal correlations only affect the term $\mathcal{C}[\partial s]$ in condition (14), which is given in equation (16). While this term appears rather complicated, it is readily computed for any special case. For illustration, we consider two scenarios.

First, assume two patches with identically and independently Bernoulli distributed selective optima, specifically, in both patches the two same selective optima 0 and 1 occur with probability 1/2. Temporal correlations are measured with a parameter $\omega_{\mathrm{T}} \in [-1, 1]$. We assume that with probability $1 - |\omega_{\mathrm{T}}|$ a selective optimum is determined according to the Bernoulli distribution, whereas with a probability $|\omega_{\mathrm{T}}|$ the selective optimum in a patch is the identical to (different from) the previous time step if $\omega_{\mathrm{T}} > 0$ ($\omega_{\mathrm{T}} < 0$). With these assumptions, it is easy to see that $\mathrm{E_T}[\mathrm{Var_S}[\theta]] = \mathrm{Var_T}[\mathrm{E_S}[\theta]] = 1/8$, $\mathrm{E_S}[\mathrm{Cov_T}[\theta_t, \theta_{t+\tau}]] = {\omega_{\mathrm{T}}}^{\tau}/4$, and $\mathrm{Cov_T}[\mathrm{E_S}[\theta_{it}], \mathrm{E_S}[\theta_{it+\tau}]] = {\omega_{\mathrm{T}}}^{\tau}/8$. The branching condition, equation (14), then equals

$$\frac{1+\gamma}{8} + \frac{\omega_{\mathrm{T}}(1-\gamma)(1-m)}{4(1-\omega_{\mathrm{T}}(1-m(1-\gamma)))} > \sigma^2. \tag{C21}$$

This relation is plotted in figure 2A for parameter values $\omega_{\mathrm{T}} = 0$ (solid line), $\omega_{\mathrm{T}} = 0.3, 0.6, 0.9$ (dotted lines, bottom to top) and $\omega_{\mathrm{T}} = -0.3, -0.6, -0.9$ (dashed lines, top to bottom).

Second, we consider a scenario in which the probability distributions differ between patches. In particular, we still assume that there are two Bernoulli distributed patches with possible optima 0 and 1, but now we take the probability of occurrence of optimum 1 to be 1/3 and 2/3 in patch one and two, respectively. Modeling temporal autocorrelation in the same way as above, we can compute the terms in equation (15), which yields $\mathrm{E_T}[\mathrm{Var_S}[\theta]] = 5/36$, $\mathrm{Var_T}[\mathrm{E_S}[\theta]] = 4/9$, $\mathrm{Var_S}[\mathrm{E_T}[\theta]] = 1/36$, $\mathrm{E_S}[\mathrm{Cov_T}[\theta_t, \theta_{t+\tau}]] = 2{\omega_{\mathrm{T}}}^{\tau}/9$, and $\mathrm{Cov_T}[\mathrm{E_S}[\theta_t], \mathrm{E_S}[\theta_{t+\tau}]] = {\omega_{\mathrm{T}}}^{\tau}/9$. Hence, the branching condition becomes

$$\frac{5}{36} + \frac{4\gamma}{9} + \frac{1-m}{18m} + \frac{2\omega_{\mathrm{T}}(1-\gamma)(1-m)}{9(1-\omega_{\mathrm{T}}(1-m(1-\gamma)))} > \sigma^2. \tag{C22}$$

This relation is plotted in figure 2B for parameter values $\omega_{\mathrm{T}} = 0$ (solid line), $\omega_{\mathrm{T}} = 0.3, 0.6, 0.9$ (dotted lines, bottom to top) and $\omega_{\mathrm{T}} = -0.3, -0.6, -0.9$ (dashed lines, top to bottom).

C.4. Protected polymorphism

In this appendix, we show that, as soon as the left-hand side of our branching condition (equation 14) is positive, pairs of trait values can be found that are able to coexist in a protected dimorphism. However, at least locally around the singular point x^*, if inequality (14) is not fulfilled, such a dimorphism can be invaded and replaced by the singular strategy. We consider the case of Gaussian selection.

Metz et al. (1996) and Geritz et al. (1998) showed that singular points in one-dimensional trait spaces can generically be classified into eight different configurations. These configurations can be visualized in terms of pairwise invasibility plots (PIPs, figure C1A,B). In our model, four out of these eight configurations are impossible. To see this, note that in our model the singular point is always an attractor of the evolutionary dynamics (cf. appendix C). In terms of PIPs, this means that to the left of the singular point we have a plus-region above the diagonal and a minus-region below the diagonal while to the right of the singular point this pattern is reversed. This rules out four of the possible eight configurations. From the remaining four configurations only two allow for protected dimorphism (figure C1A,B). For these PIPs, one can show that the set of pairs of types that are able to coexist locally around a singular point is non-empty (figure C1C,D). Mathematically speaking, this is the case if and only if

$$\left.\frac{\partial^2 w(y,x^*)}{\partial y^2}\right|_{y=x^*} > -\left.\frac{\partial^2 w(x^*,x)}{\partial x^2}\right|_{x=x^*} \tag{C23}$$

(Metz et al. 1996; Geritz et al. 1998). The left-hand side in this inequality is given by equation (B27) and the right-hand side takes an analogous form where all derivatives with respect to y are replaced by derivatives with respect to x. The derivatives $(\partial_y \rho_{it})^*$ appearing in equation (B27) are given by equations (B28) and (B30). Analogously, we obtain

$$(\partial_x \rho_{it})^* = -\frac{\theta_{it} - x^*}{\sigma^2} \tag{C24}$$

and

$$(\partial_x^2 \rho_{it})^* = \frac{(\theta_{it} - x^*)^2}{\sigma^4} + \frac{1}{\sigma^2}. \tag{C25}$$

Inserting these expressions into inequality (C23) we obtain

$$2\sigma_{\text{crit}}^2 > 0, \tag{C26}$$

where σ_{crit}^2 is the left-hand side of condition (15). Thus, in our model, if the the left-hand side of equation (14) is positive,, then pairs of types that are located symmetrically around the singular point can surely coexist in a protected dimorphism. We can see from figure C1 that coexistence is not restricted to symmetric pairs but is possible, depending on parameter values, also for pairs that are slightly asymmetric (figure C1C) or even for pairs that are located on the same side of the singular point (figure C1D). Note, that the case of $\sigma_{\text{crit}}^2 = 0$ corresponds to the degenerate

configuration where the non-diagonal zero-contour line in the PIP has a slope of $-45°$. In this case, the set of pairs of types that can coexist locally around a singular point is empty and types that are located exactly symmetrically around the singular point are selectively neutral with respect to each other.

How do the two possible configurations of singular points differ from each other? The PIP in figure C1A shows a singular point that is uninvadable (condition 15 not fulfilled) while the PIP in figure C1B shows a singular point that is invadable by nearby mutants and thus shows an evolutionary branching point (condition 15 fulfilled). From the classification of singular points it is also known that locally around a singular point the direction of the coevolutionary dynamics of two coexisting types points towards the singular strategy if the singular point is uninvadable (figure C1C). That is, selection is convergent in this case, while selection is divergent if the singular point is a branching point (figure C1D). Thus, in the first case a polymorphism is protected only on the ecological timescale but not on the evolutionary timescale where the polymorphism is expected to be eventually replaced by a single phenotype adopting the singular strategy. If, however, the singular point is a branching point, then a protected dimorphism can emerge from a monomorphism. Furthermore, the types present in the dimorphism are expected to subsequently evolve away from each other leading to increased genetic variance.

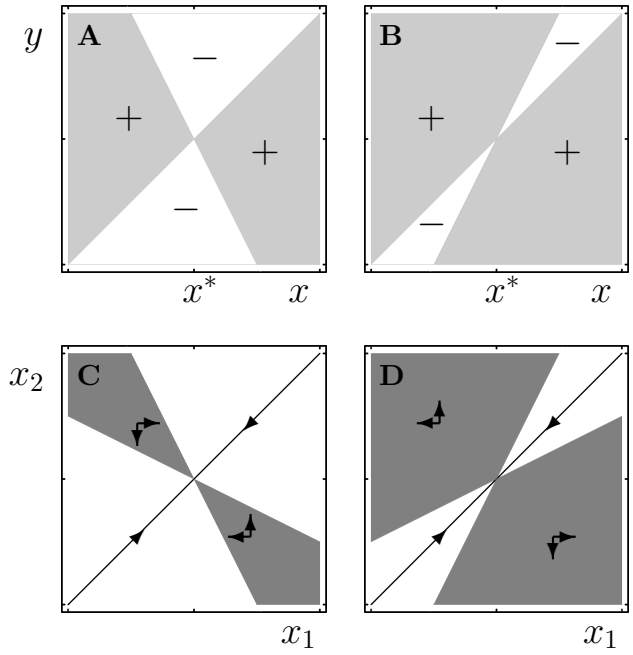

Fig. C1.— (A, B) Representative pairwise invadability plots (PIPs) for the two types of singular points allowing for protected dimorphism that are possible in our model. PIPs are contour plots of the invasion fitness function $w(y, x)$ with a single contour line at height zero. The abscissa gives the resident trait value x and the ordinate gives the mutant trait value y. Combinations of resident and mutant trait values located in the gray region, labelled with $+$, indicate that for these types $w(y, x) > 0$ while combinations of resident and mutant trait values located in the white region, labelled with $-$, indicate that for these two types $w(y, x) < 0$. Panel A shows a singular point that is an attractor of the evolutionary dynamics and uninvadable by nearby mutants and thus an evolutionary endpoint. Panel B shows a singular point that is an evolutionary branching point. (C,D) Coexistence plots for two types in the neighborhood of the singular point x^* corresponding to the PIPs directly above. These plots can be derived by plotting the contour plots for $w(y, x)$ and $w(x, y)$ on top of each other. The abscissa gives the trait value x_1 of one type and the ordinate gives the trait value x_2 of a second type. Combinations of types where $w(x_1, x_2) > 0$ and $w(x_2, x_1) > 0$, i.e., where the two types can coexist in a protected dimorphism, are shown gray. Arrows indicate the direction of gradual evolutionary change. The arrows on the diagonal indicate that for $x_1 = x_2$, i.e., for monomorphic evolution, the singular point is an attractor in both cases. For more information about the use of PIPs to derive the direction of monomorphic and dimorphic evolution see Metz et al. (1996), Geritz et al. (1998) and Diekmann (2004).

D. Online Supplementary: Additional methods and results

D.1. Numerical calculation of σ^2_{crit}

To check the accuracy of our analytical formulas, we also calculate σ^2_{crit} numerically. For this, we compute invasion fitness of a mutant close to the resident located at the singular point for different values of σ^2 and check below which value of σ^2 invasion fitness is positive and the fitness landscape thus has a local minimum at the singular point. Invasion fitness is calculated using the procedure given in Metz (2008) and, for given parameters, σ^2_{crit} is numerically approached using a method of nested intervals. The commented Mathematica (Wolfram Research, Inc. 2011) source code is given in online appendix D.4.

In Figure D1 we compare some of our analytical results from figure 2A to numerical calculations. We find that the results are in close agreement. This is also true for figure 2B (not shown). Discrepancy only occurs for very strong temporal correlation (not shown) and for very small dispersal probabilities (figure D1B). The former represents the fact that for the numerical calculation we approximate the infinite time average by a long time series and that this approximation becomes increasingly unreliable as temporal correlations increase. The latter stems from a discrepancy between the assumptions in the analytical and numerical approaches: In the analytical treatment we derive a condition for disruptive selection locally around the singular point, but for the numerical calculations we need to assume a discrete distance between mutant and resident. In the case of identically distributed patches, the range of mutants that can coexist with the singular strategy decreases with decreasing dispersal probability m. As a consequence, the numerical value of σ^2_{crit} is smaller than predicted by the analytical results for very small m. This effect becomes stronger the larger the distance between mutant and resident in the numerical calculations (figure D1B).

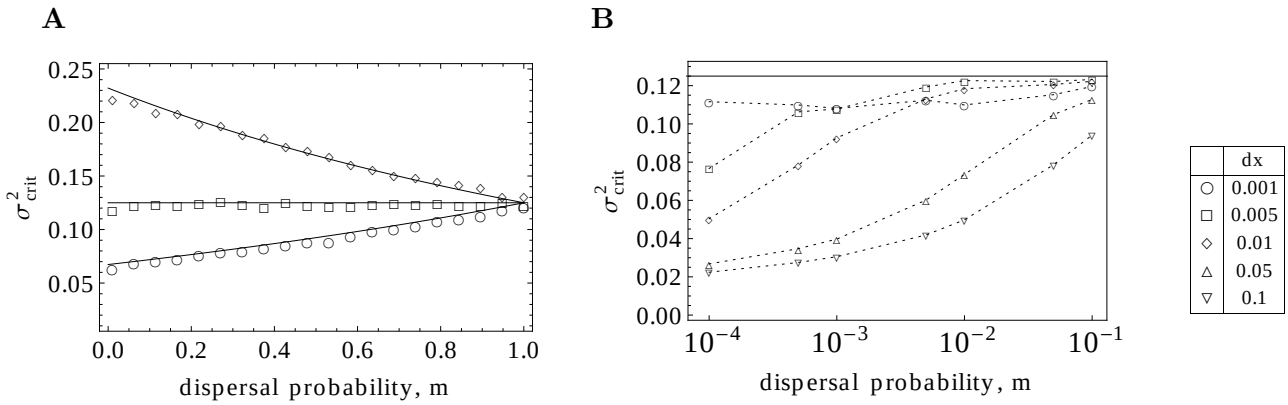

Fig. D1.— Critical strength of selection below which selection is disruptive as a function of the dispersal probability, m. We assume two independently identically Bernoulli distributed patches. (A) We compare the analytical formula for σ^2_{crit} (lines, equation C21) to numerical calculations (plot markers). Circles, squares and diamonds correspond to a coefficient of temporal correlation of $\omega_{\text{T}} = -0.3$, 0 and 0.3, respectively. Generally the results are in good agreement, except for very small m. (B) Here, we concentrate on the case without temporal correlations and zoom into the parameter region of very small m (log-scale). The different plot markers vary the distance dx between resident at the singular point and mutant. The horizontal solid line gives the analytical expectation. The critical strength of selection decreases with m for very small m. This effect becomes stronger as dx increases. Parameters: Each data point averaged over 300 runs in (A) and 100 runs in (B). (A,B) $T = 10^5$, $\gamma = 0$. Other parameter values as given in online appendix D.4.

D.2. Individual based simulations

Extensive individual based computer simulations are performed for two main reasons: (1) The robustness of all analytical results is tested against violation of the adaptive dynamics assumptions. In particular, we investigate the effect of population size, mutation rate, mutational effect size, mode of reproduction and number of loci. (2) The structure of the genetic polymorphism after branching is investigated. Simulations are performed on the Vienna Scientific Cluster (VSC) using Matlab R2011a (Mathworks 2011). The commented source code of the simulation function is given in section D.5.

The implementation of the model follows closely the model description given in the main text. It can be summarized by the following steps. For each adult individual, a random draw determines whether it survives to the next time step or dies. The number of offspring gametes of each adult is determined according to equation (1), where the trait of an individual is the sum of the values at each locus. We assume that each locus can take a set of discrete values on the real axis. The distance

between two values is a parameter – the minimal mutational step size. We assume that the loci are equally spaced on linear chromosomes. From the total number of offspring gametes in each patch, we draw the gametes that replace the dying adult individuals. All other offspring die. With a certain probability, the surviving gametes are the product of one or more recombination events between the parental chromosomes. The surviving gametes of each patch fuse to form diploids. With a certain probability, the values at a locus of an individual have undergone mutation. Mutations are drawn from a Gaussian distribution with a certain variance and are rounded to the minimal mutational step size. We also investigate the case of fixed mutational step-sizes. With probability m the newly established individuals disperse globally between patches (note that we assume that $k_i = c_i$). Alternatively, we also investigate the case that gametes disperse instead of zygotes; we do not detect any difference in the results. We also treat the case of haploid clonal reproduction where the steps of gamete fusion and recombination are simply omitted.

We investigate many different parameter combinations. Table 3 gives an overview of the most important parameters. The total set of parameters is commented in the source code below. The most important results of the simulation study are discussed in the second half of the results section.

D.3. Supplementary figures

To restrict the parameter space, all simualtion figures in the main text assumed full dispersal ($m = 1$). Figure D2 investigates the accuracy of the analytical branching conditions for different values of the dispersal parameter. The observed increase in genetic variance in the simulation study generally matches the branching condition. For identically distributed patch optima and very low dispersal (figure D2A, $m < 0.1$) the increase in genetic variance is rather slow and the accuracy is thus difficult to judge. A possible reason for this is that the maximum phenotypic distance between genotypes that can coexist decreases with decreasing m (cf. figure D1B) and that environmental stochasticity is strong in such a scenario.

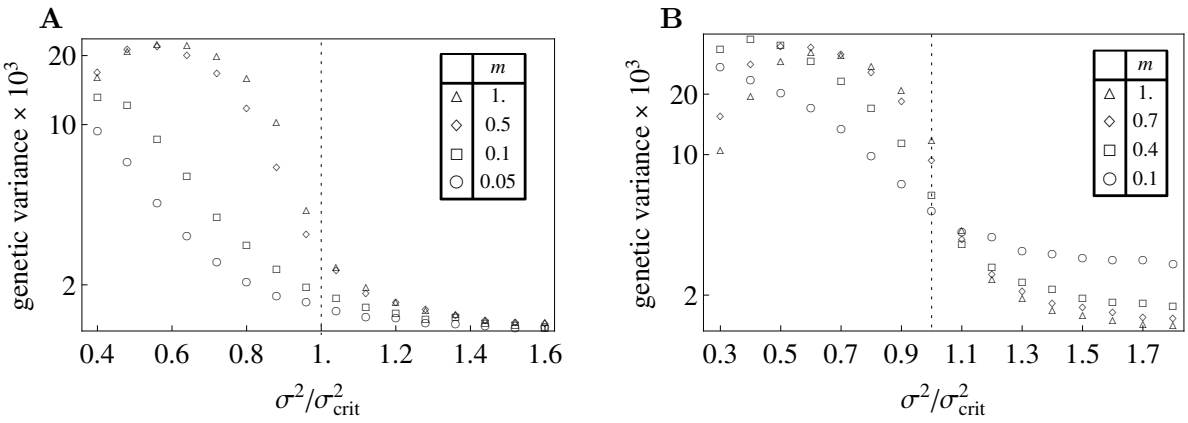

Fig. D2.— Long-term average genetic variance (on log-scale) measured from individual based simulations as a function of the strength of Gaussian stabilizing selection for (A) identically and (B) differently distributed selective optima across two patches (cf. figure 2A vs. B). Spatial and temporal correlations are absent. Recall that for different environmental distributions (panel B) σ^2_{crit} depends on m, while for identically distributed patch optima (panel A) it is independent of m. The dotted vertical line indicates the analytically expected branching point $\sigma^2/\sigma^2_{\text{crit}} = 1$ (cf. equation 15). The analytical condition for evolutionary branching matches with the observed increase in genetic variance in individual based simulations. As an exception, for identically distributed patches and very low dispersal (panel A, $m \leq 0.1$, squares & circles) the precise onset of the increase in genetic variance is difficult to judge and the amount of genetic variation is significantly reduced. Parameter values: $\gamma = 0$, $k = 2$, $rec = 0.05$, $\mu_{\text{trait}} = 0.001$; other parameters as given in table 3.

Figure D3 and D4 show additional simulation runs investigating the influence of population size on branching. The plots are analogous to figure 6A and figure 6B, respectively, except for some parameter variations. See plot legends for details. Overall, the results are very similar to figure 6. As an exception, we observe that in the case of lower mutation rates and smaller mutational effect sizes, deviations from our branching conditions appear already for smaller total population sizes (figure D3A).

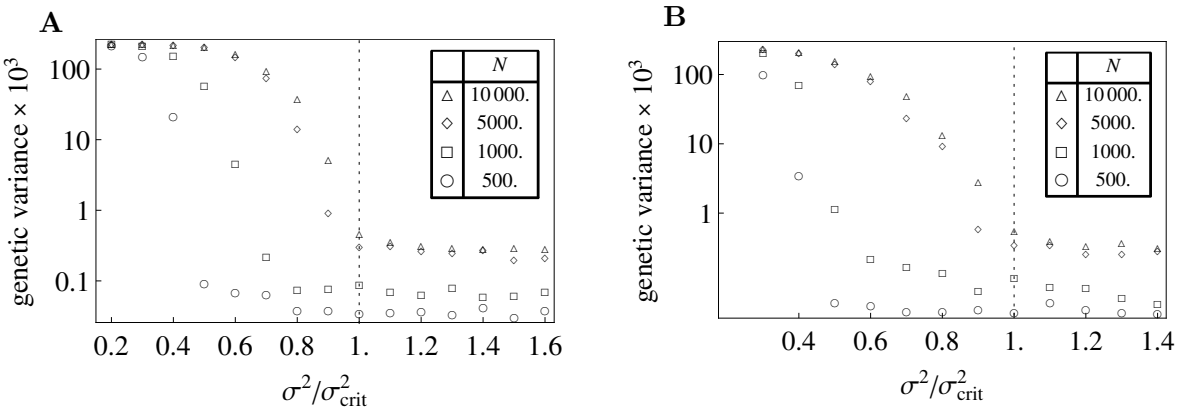

Fig. D3.— Long-term average genetic variance in a population (on log-scale) from individual-based simulations as a function of the strength of Gaussian stabilizing selection for different population sizes. The plots are equivalent to figure 6A except for the following parameter variations. Panel (A) assumes lower mutation rate ($\mu_{\text{trait}} = 0.001$) and smaller mutational effect-size ($\sigma_\mu = 0.01$). Panel (B) assumes differently distributed selective optima across patches (cf. figure 2B), a lower dispersal probability ($m = 0.5$) and a higher number of patches ($n = 10$). (A) For smaller mutational parameters, deviations from our branching conditions appear already for $N = 1000$. (B) Results are similar to 6A. Parameter values: (A) $\gamma = 0.5$, (B) $\gamma = 0$; other parameters as in figure 6A.

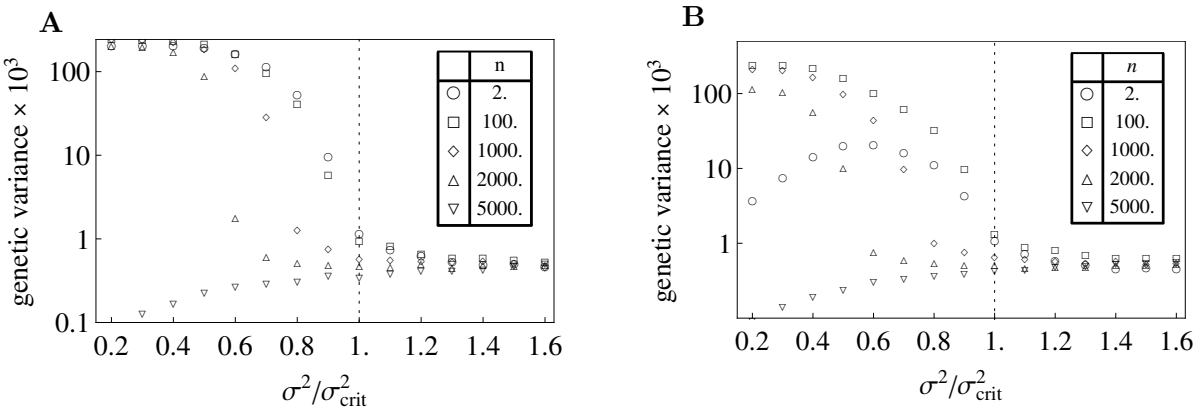

Fig. D4.— Long-term average genetic variance in a population (on log-scale) as a function of the strength of Gaussian stabilizing selection for different patch numbers at a constant total population size. The plots are equivalent to figure 6B except for the following parameter variations. Panel (A) assumes lower mutation rate ($\mu_{\text{trait}} = 0.001$) and smaller mutational effect-size ($\sigma_\mu = 0.01$). In panel (B) generation overlap is absent ($\gamma = 0$). Results are qualitatively similar to figure 6B. Deviations from the branching condition can only be detected for very small local population sizes ($n > 1000$, less than 10 individuals per patch). We added a data point for two individuals per patch ($n = 5000$). Under these conditions there is no negative frequency dependence and thus no adaptive genetic polymorphism. Other parameter values as in figure 6B.

D.4. Source code for numerical calculations

Below we give the source code used for numerical calculations of σ^2_{crit} using Mathematica (Wolfram Research, Inc. 2011). Lines 4-5 give the definition of $r(x, \theta_{it})$ (equation 1) and lines 11-16 give the definition of $\mathsf{L}(x, \phi_{1t}, .., \phi_{nt}, \theta_{1t}, .., \theta_{nt})$ (equations 4a and 4b). Note that we use $\Theta = (\theta_1, .., \theta_n)$. Lines 20-32 define a function that computes $w(y, x)$ (the variables are called xm and xr) with the method described in Metz (2008) and lines 38-47 give a function using a nested intervals method to calculate σ^2_{crit} for given parameter values. Explanation of the parameters and variables are given as comments in the code above each function. Note that the function to calculate σ^2_{crit} presented here assumes that there are no temporal and spatial correlations. Adapting the function to a given type of correlations is straight forward. Lines 51-54 give a typical calculation of the critical strength of selection as a function of the dispersal probability m. If not otherwise stated the given parameters are used for all calculations.

[Please refer to the online supplementary of the pubslished version for the source code, or contact the authors directly.]

D.5. Source code for individual based simulations

In the following, we give the source code of the individual based simulation function, written in Matlab (Mathworks 2011). Note that the source code presented here is optimized for readability rather that computational efficiency. For instance, clonal haploid and sexual diploid reproduction are given in a single function.

[Please refer to the online supplementary of the pubslished version for the source code, or contact the authors directly.]

REFERENCES

Abrams, P. A., H. Matsuda, and Y. Harada. 1993. Evolutionary unstable fitness maxima and stable fitness minima of continuous traits. Evolutionary Ecology 7:465–487.

Abrams, P. A., C. M. Tucker, and B. Gilbert. 2013. Evolution of the storage effect. Evolution 67:315–327.

Ajar, E. 2003. Analysis of disruptive selection in subdivided populations. Bmc Evolutionary Biology 3:22.

Bergelson, J., M. Kreitman, E. A. Stahl, and D. C. Tian. 2001. Evolutionary dynamics of plant r-genes. Science 292:2281–2285.

Bolnick, D. I., R. Svanbäck, J. A. Fordyce, L. H. Yang, J. M. Davis, C. D. Hulsey, and M. L. Forister. 2003. The ecology of individuals: Incidence and implications of individual specialization. The American Naturalist 161:1–28.

Byers, D. L. 2005. Evolution in heterogeneous environments and the potential of maintenance of genetic variation in traits of adaptive significance. Genetica 123:107–124.

Chesson, P. L. 1984. The storage effect in stochastic population models. Lecture Notes in Biomathematics 54:76–89.

———. 1985. Coexistence of competitors in spatially and temporally varying environments - a look at the combined effects of different sorts of variability. Theoretical Population Biology 28:263–287.

———. 1994. Multispecies competition in variable environments. Theoretical Population Biology 45:227–276.

———. 2000*a*. General theory of competitive coexistence in spatially-varying environments. Theoretical Population Biology 58:211–237.

———. 2000*b*. Mechanisms of maintenance of species diversity. Annual Review of Ecology and Systematics 31:343–368.

Chesson, P. L., and R. R. Warner. 1981. Environmental variability promotes coexistence in lottery competitive systems. The American Naturalist 117:923–943.

Christiansen, F. B. 1974. Sufficient conditions for protected polymorphism in a subdivided population. The American Naturalist 108:157–166.

———. 1975. Hard and soft selection in a subdivided population. American Naturalist 109:11–16.

Claessen, D., J. Andersson, L. Persson, and A. de Roos. 2007. Delayed evolutionary branching in small populations. Evolutionary Ecology Research 9:51–69.

Comins, H. N., and I. R. Noble. 1985. Dispersal, variability, and transient niches - species coexistence in a uniformly variable environment. The American Naturalist 126:706–723.

Cook, L. M. 2003. The rise and fall of the carbonaria form of the peppered moth. Quarterly Review of Biology 78:399–417.

Cook, R. D., and D. J. Hartl. 1974. Uncorrelated random environments and their effects on gene frequency. Evolution 28:265–274.

Day, T. 2000. Competition and the effect of spatial resource heterogeneity on evolutionary diversification. The American Naturalist 155:790–803.

———. 2001. Population structure inhibits evolutionary diversification under competition for resources. Genetica 112-113:71–86.

Deakin, M. A. B. 1966. Sufficient conditions for genetic polymorphism. The American Naturalist 100:690–692.

———. 1968. Genetic polymorphism in a subdivided population. Australian Journal of Biological Sciences 21:165–168.

Débarre, F., and S. Gandon. 2010. Evolution of specialization in a spatially continuous environment. J Evol Biol 23:1090–1099.

———. 2011. Evolution in heterogeneous environments: between soft and hard selection. The American Naturalist 177:E84–E97.

Dempster, E. R. 1955. Maintenance of genetic heterogeneity. Cold Spring Harb Symp Quant Biol 20:25–31.

Dieckmann, U., and M. Doebeli. 1999. On the origin of species by sympatric speciation. Nature 400:354–357.

Dieckmann, U., and R. Law. 1996. The dynamical theory of coevolution: A derivation from stochastic ecological processes. Journal of Mathematical Biology 34:579–612.

Diekmann, O. 2004. A beginners guide to adaptive dynamics. Pages 47–86 *in* R. Rudnicki, ed. Mathematical Modelling of Population Dynamics, vol. 63 of *Banach Center Publications*. Polish Academy of Sciences, Warszawa.

Ellner, S., and N. G. Hairston. 1994. Role of overlapping generations in maintaining genetic variation in a fluctuating environment. The American Naturalist 143:403–417.

Eshel, I. 1983. Evolutionary and continuous stability. Journal of Theoretical Biology 103:99–111.

Felsenstein, J. 1976. The theoretical population genetics of variable selection and migration. Annual Review in Genetics 10:253–280.

Geritz, S., É. Kisdi, G. Meszéna, and J. Metz. 1998. Evolutionarily singular strategies and the adaptive growth and branching of the evolutionary tree. Evolutionary Ecology 12:35–57.

Geritz, S. A. H. 2005. Resident-invader dynamics and the coexistence of similar strategies. Journal of Mathematical Biology 50:67–82.

Gillespie, J. 1973*a*. Natural-selection with varying selection coefficients - haploid model. Genetical Research 21:115–120.

Gillespie, J., and C. Langley. 1976. Multilocus behavior in random environments. 1. Random levene models. Genetics 82:123–137.

Gillespie, J., and M. Turelli. 1989. Genotype-environment interactions and the maintenance of polygenic variation. Genetics 121:129–138.

Gillespie, J. H. 1973*b*. Polymorphism in random environments. Theoretical Population Biology 4:193–195.

———. 1974. Polymorphism in patchy environments. The American Naturalist 108:145–151.

———. 1975. Role of migration in genetic structure of populations in temporarily and spatially varying environments. 1. Conditions for polymorphism. The American Naturalist 109:127–135.

———. 1976. Role of migration in genetic structure of populations in temporally and spatially varying environments. 2. Island models. Theoretical Population Biology 10:227–238.

Gliddon, C., and C. Strobeck. 1975. Necessary and sufficient conditions for multiple-niche polymorphism in haploids. The American Naturalist 109:233–235.

Hedrick, P. W. 1978. Genetic-variation in a heterogeneous environment. 5. Spatial heterogeneity in finite populations. Genetics 89:389–401.

———. 2006. Genetic polymorphism in heterogeneous environments: The age of genomics. Annual Review of Ecology, Evolution and Systematics 37:67–93.

Hedrick, P. W., M. E. Ginewan, and E. P. Ewing. 1976. Genetic-polymorphism in heterogeneous environments. Annual Review of Ecology and Systematics 7:1–32.

Houle, D. 1992. Comparing evolvability and variability of quantitative traits. Genetics 130:195–204.

Johansson, J., and J. Ripa. 2006. Will sympatric speciation fail due to stochastic competitive exclusion? American Naturalist 168:572–578.

Johansson, J., J. Ripa, and N. Kucklander. 2010. The risk of competitive exclusion during evolutionary branching: Effects of resource variability, correlation and autocorrelation. Theoretical Population Biology 77:95–104.

Karlin, S. 1982. Classifications of selection migration structures and conditions for a protected polymorphism. Evolutionary Biology 14:61–204.

Karlin, S., and B. Levikson. 1974. Temporal fluctuations in selection intensities - case of small population-size. Theoretical Population Biology 6:383–412.

Kassen, R. 2002. The experimental evolution of specialists, generalists, and the maintenance of diversity. Journal of Evolutionary Biology 15:173–190.

Kimura, M. 1954. Process leading to quasi-fixation of genes in natural populations due to random fluctuation of selection intensities. Genetics 39:280–295.

———. 1955. Stochastic processes and distribution of gene frequencies under natural selection. Cold Spring Harbor Symposia On Quantitative Biology 20:33–53.

Kisdi, É. 2002. Dispersal: Risk spreading versus local adaptation. The American Naturalist 159:579–596.

Kisdi, É., and S. A. H. Geritz. 1999. Adaptive dynamics in allele space: Evolution of genetic polymorphism by small mutations in a heterogeneous environment. Evolution 53:993–1008.

Kopp, M., and J. Hermisson. 2006. The evolution of genetic architecture under frequency-dependent disruptive selection. Evolution 60:1537–1550.

Leimar, O. 2005. The evolution of phenotypic polymorphism: Randomized strategies versus evolutionary branching. The American Naturalist 165:669–681.

———. 2008. Environmental and genetic cues in the evolution of phenotypic polymorphism. Evolutionary Ecology .

Leimar, O., T. J. M. Van Dooren, and P. Hammerstein. 2006. A new perspective on developmental plasticity and the principles of adaptive morph determination. The American Naturalist 167:367–376.

Levene, H. 1953. Genetic equilibrium when more than one ecological niche is available. The American Naturalist 87:331–333.

Levins, R. 1962. Theory of fitness in a heterogeneous environment. I. The fitness set and the adaptive function. The American Naturalist 96:361–373.

Mackay, T. F. C. 1981. Genetic-variation in varying environments. Genetical Research 37:79–93.

MathWorks, Inc. 2011. MATLAB: the language of technical computing. Desktop tools and development environment, version R2011a, vol. 7.12.0.635. MathWorks.

McKenzie, J. A. 1996. Ecological and evolutionary aspects of insecticide resistance. R. G. Landes Co., Austin, Texas, USA.

Meszéna, G., I. Czibula, and S. A. H. Geritz. 1997. Adaptive dynamics in a 2-patch environment: a toy model for allopatric and parapatric speciation. Journal of Biological Systems 5:265–284.

Metz, J. 2008. Fitness. Pages 1599–1612 *in* S. Jørgensen and B. Fath, eds. Evolutionary Ecology. Vol. [2] of Encyclopedia of Ecology. Elsevier.

Metz, J., S. Geritz, G. Meszéna, F. Jacobs, and J. Van Heerwaarden. 1996. Adaptive dynamics: A geometrical study of the consequences of nearly faithful reproduction. Pages 183–231 *in* S. van Strien and S. Verduyn Lunel, eds. Stochastic and spatial structures of dynamical systems, Proceedings of the Royal Dutch Academy of Science. North Holland, Dordrecht, Netherlands; available at http://www.iiasa.ac.at/Research/ADN/Series.html.

Metz, J., R. Nisbet, and S. Geritz. 1992. How should we define 'fitness' for general ecological scenarios? Trends in Ecology and Evolution 7:198–202.

Nachman, M. W., H. E. Hoekstra, and S. L. D'Agostino. 2003. The genetic basis of adaptive melanism in pocket mice. Proceedings of the National Academy of Sciences of the United States of America 100:5268–5273.

Nevo, E. 1978. Genetic-variation in natural-populations - patterns and theory. Theoretical Population Biology 13:121–177.

Nilsson, J., and J. Ripa. 2010*a*. Adaptive branching in source-sink habitats. Evolutionary Ecology 24:479–489.

———. 2010*b*. The origin of polymorphic crypsis in a heterogeneous environment. Evolution 64:1386–1394.

Nurmi, T., and K. Parvinen. 2008. On the evolution of specialization with a mechanistic underpinning in structured metapopulations. Theoretical Population Biology 73:222–243.

———. 2011. Joint evolution of specialization and dispersal in structured metapopulations. Journal of Theoretical Biology 275:78–92.

Parvinen, K., and M. Egas. 2004. Dispersal and the evolution of specialization in a two-habitat type metapopulation. Theoretical Population Biology 66:233–248.

Peischl, S., and K. A. Schneider. 2010. Evolution of dominance under frequency-dependent intraspecific competition in an assortatively mating population. Evolution 64:561–582.

Pelz, H. J., S. Rost, M. Hunerberg, A. Fregin, A. C. Heiberg, K. Baert, A. D. MacNicoll, C. V. Prescott, A. S. Walker, J. Oldenburg, and C. R. Muller. 2005. The genetic basis of resistance to anticoagulants in rodents. Genetics 170:1839–1847.

Pennings, P. S., M. Kopp, G. Meszéna, U. Dieckmann, and J. Hermisson. 2008. An analytically tractable model for competitive speciation. The American Naturalist 171:E44–E71.

Ravigné, V., U. Dieckmann, and I. Olivieri. 2009. Live where you thrive: Joint evolution of habitat choice and local adaptation facilitates specialization and promotes diversity. The American Naturalist 174:E141–E169.

Rueffler, C., T. J. M. Van Dooren, O. Leimar, and P. A. Abrams. 2006. Disruptive selection and then what? Trends in Ecology and Evolution 21:238–245.

Schreiber, S. J. 2010. Interactive effects of temporal correlations, spatial heterogeneity and dispersal on population persistence. Proceedings of the Royal Society B 277:1907–1914.

Seger, J., and H. J. Brockmann. 1987. What is bet-hedging? Oxford Surveys in Evolutionary Biology 4:182–211.

Snyder, R. E., and P. Chesson. 2003. Local dispersal can facilitate coexistence in the presence of permanent spatial heterogeneity. Ecology Letters 6:301–309.

Spichtig, M., and T. J. Kawecki. 2004. The maintenance (or not) of polygenic variation by soft selection in heterogenous environments. The American Naturalist 164:70–84.

Spurgin, L. G., and D. S. Richardson. 2010. How pathogens drive genetic diversity: Mhc, mechanisms and misunderstandings. Proceedings of the Royal Society B 277:979–988.

Svardal, H., C. Rueffler, and J. Hermisson. 2011. Comparing environmental and genetic variance as adaptive response to fluctuating selection. Evolution 65:2492–2513.

Szilagyi, A., and G. Meszena. 2010. Coexistence in a fluctuating environment by the effect of relative nonlinearity a minimal model. Journal of Theoretical Biology 267:502–512.

Taylor, J. E. 2008. Environmental variation, fluctuating selection and genetic drift in subdivided populations. Theoretical Population Biology 74:233–250.

Tuljapurkar, S. 1990. Population Dynamics in variable environments, vol. 85 of *Lecture Notes in Biomathematics*. Springer Verlag, Berlin, Germany.

Van Dooren, T. J. M. 1999. The evolutionary ecology of dominance. Journal of Theoretical Biology 198:519–532.

van Doorn, G., and U. Dieckmann. 2006. The long-term evolution of multilocus traits under frequency-dependent disruptive selection. Evolution 60:2226–2238.

van Doorn, S. G., U. Dieckmann, and F. J. Weissing. 2004. Sympatric speciation by sexual selection: A critical re-evaluation. The American Naturalist 163:709–725.

Via, S., and R. Lande. 1987. Evolution of genetic-variability in a spatially heterogeneous environment - effects of genotype-environment interaction. Genetical Research 49:147–156.

Vignieri, S. N., J. G. Larson, and H. E. Hoekstra. 2010. The selective advantage of crypsis in mice. Evolution 64:2153–2158.

Wakano, J. Y., and Y. Iwasa. 2013. Evolutionary branching in a finite population: Deterministic branching vs. stochastic branching. Genetics 193:229–241.

Wallace, B. 1975. Hard and soft selection revisited. Evolution 29:465– 473.

West-Eberhard, M. J. 2003. Developmental Plasticity and Evolution. Oxford University Press.

Wolfram Research, Inc. 2011. Mathematica Edition: Version 8.0. Champaign, IL.

Wright, S. 1943. Isolation by distance. Genetics 28:114–138.

———. 1948. On the roles of directed and random changes in gene frequency in the genetics of populations. Evolution 2:279–294.

Yeaman, S., and M. C. Whitlock. 2011. The genetic architecture of adaptation under migration-selection balance. Evolution 65:1897–1911.

This preprint was prepared with the AAS LaTeX macros v5.2.